Chapter 17

The Kerr solution.

17.1 The Kerr metric in the original form.

By Roy Kerr's own account [187, 188], the Kerr metric emerged during an investigation of algebraically special[55] vacuum solutions of Einstein's equations, with the intention to find a physically meaningful generalisation of the Schwarzschild solution. Then, it was found to describe the exterior gravitational field of a rotating body. No exact solution of Einstein's equations with a perfect fluid source is known that could be matched to the Kerr metric. Thus, the main application of this metric is to the description of rotating black holes. No invariant criterion leading uniquely to it is known.

Deriving the Kerr metric from the Einstein equations would require too much space as for a short course. See Refs. [187, 188] and [189] for derivations by two different methods; both methods are presented in Ref. [11]. It is one of vacuum solutions of Einstein's equations whose metrics can be transformed to the Kerr – Schild form [187]:

$$g_{\mu\nu} = \eta_{\mu\nu} - l_\mu l_\nu, \tag{17.1}$$

where $\eta_{\mu\nu}$ is the Minkowski metric in any coordinates, and l_μ is a vector field that is null with respect to $g_{\mu\nu}$. It follows that l_μ is null with respect to $\eta_{\mu\nu}$ as well, and that the inverse metric has the form

$$g^{\mu\nu} = \eta^{\mu\nu} + l^\mu l^\nu. \tag{17.2}$$

[187] R. P. Kerr and A. Schild, in *Atti del Convegno sulla Relatività Generale: Problemi dell'Energia e Onde Gravitazionali.* G. Barbera Editore, Firenze 1965, pp. 1. Reprinted in *Gen. Relativ. Gravit.* **41**, 2485 (2009), with an editorial note by A. Krasiński, E. Verdaguer and R. P. Kerr, *Gen. Relativ. Gravit.* **41**, 2469 (2009) and authors' biographies by A. Krasiński, *Gen. Relativ. Gravit.* **41**, 2482 (2009) (Kerr); and L. Shepley, *Gen. Relativ. Gravit.* **8**, 955 (1977) (Schild).

[188] R. P. Kerr and A. Schild, in *Golden Oldies in general relativity. Hidden gems.* Edited by A. Krasiński, G. F. R. Ellis, M. A. H. MacCallum, Springer, Heidelberg 2013, p. 439.

[55] Algebraically special means that its Weyl tensor has at least one repeated principal null direction – see Sec. 10.7 here and Ref. [11].

[189] B. Carter, in: *Black holes – les astres occlus.* Edited by C. de Witt and B. S. de Witt. Gordon and Breach, New York, London, Paris 1973, p. 61. Reprinted in *Gen. Relativ. Gravit.* **41**, 2874 (2009), with an editorial note by N. Kamran and A. Krasiński, *Gen. Relativ. Gravit.* **41**, 2867 (2009) and author's (auto)biography by B. Carter, *Gen. Relativ. Gravit.* **41**, 2870 (2009).

The Kerr solution was first announced [190] in the following form:[56]

$$\begin{aligned} \mathrm{d}s^2 &= \mathrm{d}t^2 - \mathrm{d}x^2 - \mathrm{d}y^2 - \mathrm{d}z^2 \\ &- \frac{2mr^3}{r^4 + a^2z^2}\left[\mathrm{d}t + \frac{z}{r}\mathrm{d}z + \frac{r}{r^2+a^2}(x\mathrm{d}x + y\mathrm{d}y) + \frac{a}{r^2+a^2}(x\mathrm{d}y - y\mathrm{d}x)\right]^2, \end{aligned} \tag{17.3}$$

where m and a are arbitrary constants and the function $r(x,y,z)$ is defined by

$$\frac{x^2+y^2}{r^2+a^2} + \frac{z^2}{r^2} = 1. \tag{17.4}$$

This metric is the simplest exact solution of Einstein's equations that describes the exterior field of a rotating body (see below). Consequently, it became a basis for hundreds of papers discussing astrophysical aspects of black holes. Also, it is believed to be the unique asymptotic state toward which all nonstationary uncharged black holes should evolve.

17.2 Basic properties.

The Kerr metric becomes the Minkowski metric when $m = 0$. It becomes approximately flat when r is large – the Kerr–Schild term in the second line of (17.3) becomes then negligible compared to the Lorentzian part. The equation

$$g_{00} = 1 - \frac{2mr^3}{r^4 + a^2z^2} \approx 1 - \frac{2m}{r} + \frac{2ma^2z^2}{r^5} + O(1/r^5), \tag{17.5}$$

shows that m is the mass of the source. A refined investigation that we shall omit here revealed that a is the total angular momentum of the source per unit mass [190, 11].

The coordinates of (17.3) are not convenient in most calculations because of the complicated form of the function $r(x,y,z)$. Often, it is more practical to use r as one of the coordinates. One such coordinate system is related to the coordinates of (17.3) by [190]

$$\begin{aligned} x &= (r\cos\varphi + a\sin\varphi)\sin\vartheta \equiv \sqrt{r^2+a^2}\sin\vartheta\cos[\varphi - \arctan(a/r)], \\ y &= (r\sin\varphi - a\cos\varphi)\sin\vartheta \equiv \sqrt{r^2+a^2}\sin\vartheta\sin[\varphi - \arctan(a/r)], \\ z &= r\cos\vartheta, \end{aligned} \tag{17.6}$$

where $r \geq 0$, $\vartheta \in [0,\pi]$, $\varphi \in [0, 2\pi]$. The transformed metric is

$$\begin{aligned} \mathrm{d}s^2 &= \mathrm{d}t^2 - \mathrm{d}r^2 - 2a\sin^2\vartheta\mathrm{d}r\mathrm{d}\varphi - \Sigma\mathrm{d}\vartheta^2 - \left(r^2+a^2\right)\sin^2\vartheta\mathrm{d}\varphi^2 \\ &- \frac{2mr}{\Sigma}\left(\mathrm{d}t + \mathrm{d}r + a\sin^2\vartheta\mathrm{d}\varphi\right)^2, \qquad \text{where} \qquad \Sigma \stackrel{\text{def}}{=} r^2 + a^2\cos^2\vartheta. \end{aligned} \tag{17.7}$$

In these coordinates the metric is independent of $x^3 = \varphi$, so $\underset{(2)}{k}{}^\alpha = \delta^\alpha_3$ is its Killing vector field. The existence of the timelike Killing field $\underset{(1)}{k}{}^\alpha = \delta^\alpha_0$ was evident already in (17.3).

[190] R. P. Kerr, *Phys. Rev. Lett.* **11**, 237 (1963).

[56] The signature in Ref. [190] was $(-,+,+,+)$; this paper did not say how the metric was derived.

The Abelian group generated by $\underset{(1)}{k}{}^{\alpha}$ and $\underset{(2)}{k}{}^{\alpha}$ is the complete symmetry group of (17.7), as can be verified by solving the Killing equations. In the Minkowski limit $m = 0$, φ becomes the azimuthal angle, so the Kerr metric is axially symmetric.

The (x, y, z) coordinates of (17.3) become Cartesian rectangular at $r \to \infty$, so they are "approximately Cartesian" at finite r. Then, the surfaces of constant r are (deformed!) confocal ellipsoids of revolution whose foci lie on the ring $\{z = 0, x^2 + y^2 = a^2\}$. On this ring $r = 0$ and $\vartheta = \pi/2$; it is a singularity of the coordinates of (17.7), and, as we shall see below, a singularity of the spacetime as well. From (17.6) it follows that

$$\frac{x^2 + y^2}{a^2 \sin^2 \vartheta} - \frac{z^2}{a^2 \cos^2 \vartheta} = 1, \tag{17.8}$$

which shows that the surfaces $\vartheta =$ constant are (deformed) one-sheeted hyperboloids of revolution, with foci on the same ring. The surface $\vartheta = \pi/2$ is the plane $z = 0$ with the ring $r = 0$ and its interior removed. Figure 17.1 shows the axial cross-section through the family of the constant-r and constant-ϑ hypersurfaces.

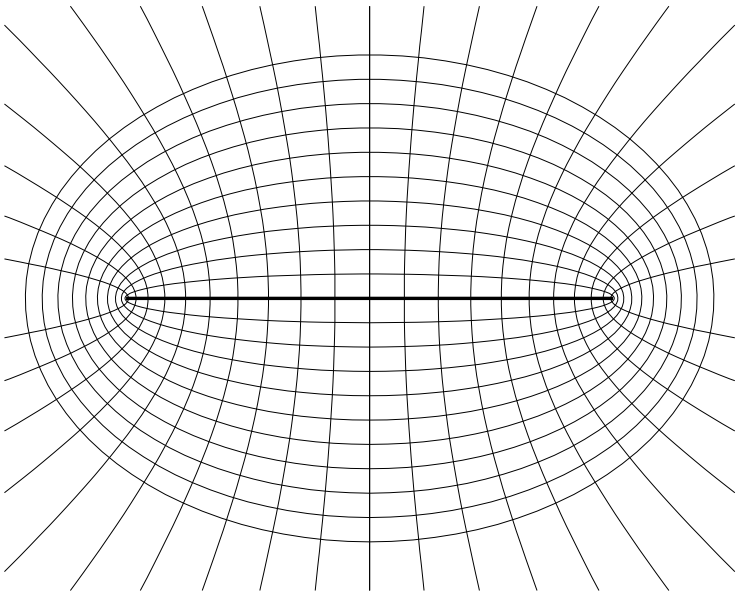

Figure 17.1: A cross-section through the space $t =$ constant by a plane containing the axis of symmetry. The figure shows the surfaces of constant r (the ellipses) and the surfaces of constant ϑ (the hyperbolae). The ellipsoids and the hyperboloids all have their foci on the ring of radius $|a|$, seen here as the thick horizontal line; it has the equation $r = 0$, $\vartheta = \pi/2$. The (r, ϑ, φ) coordinates are singular on this ring. When $\vartheta \to \pi/2$, the hyperboloid degenerates to the $z = 0$ plane with the disc $r = 0$ removed.

To visualise the $\varphi =$ constant surfaces we transform (x, y) in (17.6) by [191]

$$\xi = x \cos \varphi + y \sin \varphi, \qquad \eta = -x \sin \varphi + y \cos \varphi. \tag{17.9}$$

[191] R. H. Boyer and R. W. Lindquist, *J. Math. Phys.* **8**, 265 (1967).

Then, from (17.6)

$$(\xi = r\sin\vartheta, \quad \eta = -a\sin\vartheta) \Longleftrightarrow \left(\frac{a}{\eta}\right)^2 - \left(\frac{z}{\xi}\right)^2 = 1. \tag{17.10}$$

Since $r \geq 0$ and $\vartheta \in [0, \pi]$, we have $\xi \geq 0$ and $\eta/a \leq 0$. The coordinates ξ and η are obtained by rotating the x and y axes by the angle φ. The surface (17.10) consists of two sheets that are mirror-images of each other; the one on which $z \geq 0$, with $a > 0$, is shown in Fig. 17.2. Other $\varphi =$ constant surfaces are obtained by rotating the one in Fig. 17.2 around the z-axis. The surface contains the straight half-lines $\{z = \xi\cot\vartheta, \vartheta = \text{constant}\}$ along which it intersects the $\vartheta =$ constant hyperboloids.

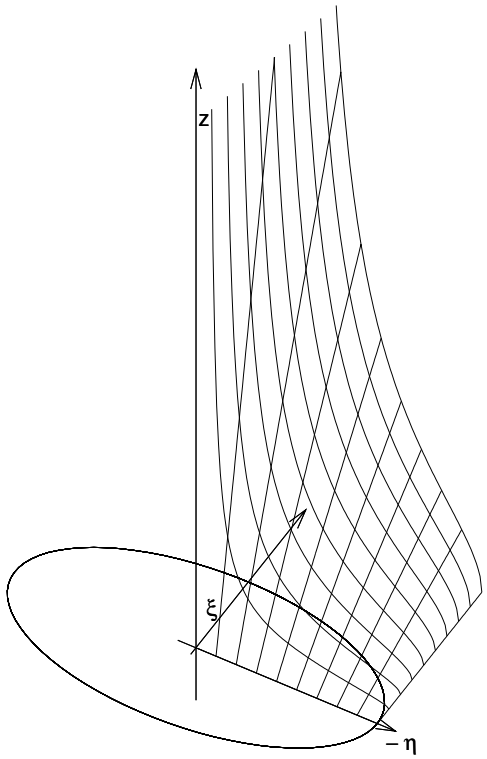

Figure 17.2: A surface of constant φ in the coordinates of (17.7). Its tangent planes become vertical at the right edge and at $z \to \infty$. The distance from the z-axis to the right edge is $|a|$. The figure shows only one half of this surface. The other half is the mirror-reflection in the $z = 0$ plane, other surfaces of constant φ are obtained by rotating this one around the z axis. The straight half-lines $\{z = \xi\cot\vartheta, \xi \geq 0\}$ seen in the figure are intersections of $\varphi =$ constant with the surfaces of constant ϑ. The η axis is drawn in reverse, so the coordinate on it is $(-\eta)$. The circle is the singular ring $\{r = |a|, \vartheta = \pi/2\}$.

A still more readable form of the Kerr metric results when the **Boyer–Lindquist (B–L) coordinates** [191] are introduced. They are related to those of (17.7) by[57]

$$t \;=\; t' + 2m\int \frac{r\mathrm{d}r}{\Delta_r(r)}, \qquad \varphi = -\varphi' - a\int \frac{\mathrm{d}r}{\Delta_r(r)}, \qquad \Delta_r(r) \stackrel{\text{def}}{=} r^2 - 2mr + a^2,$$

[57] The φ' in (17.11) and the term with $\mathrm{d}t\mathrm{d}\varphi$ in (17.12) have opposite signs to those implied by Ref. [191]. This change was made in order to be consistent with the papers referred to in subsequent sections.

$$r = r', \qquad \vartheta = \vartheta'. \tag{17.11}$$

The resulting metric, with primes dropped, is

$$\begin{aligned} \mathrm{d}s^2 &= \left(1 - \frac{2mr}{\Sigma}\right)\mathrm{d}t^2 + \frac{4mra\sin^2\vartheta}{\Sigma}\mathrm{d}t\mathrm{d}\varphi - \left(\frac{2mra^2\sin^2\vartheta}{\Sigma} + r^2 + a^2\right)\sin^2\vartheta\mathrm{d}\varphi^2 \\ &- \frac{\Sigma}{\Delta_r}\mathrm{d}r^2 - \Sigma\mathrm{d}\vartheta^2. \end{aligned} \tag{17.12}$$

The limit $a = 0$ of this is seen to be the Schwarzschild solution.

Since the B–L coordinates (r, ϑ, φ) are orthogonal in each hypersurface $t =$ constant, the surfaces $\varphi =$ constant can be imagined as planes orthogonal to the ellipsoids and to the hyperboloids. (In fact, they are only approximately planes – they are clearly nonflat.)

The Schwarzschild metric has a spurious singularity at $r = 2m$, where $g_{rr} \to \infty$ and $g_{tt} = 0$. In the Kerr metric, the set where $g_{rr} \to \infty$ (i. e., $\Delta_r = 0$) is different from $g_{tt} = 0$. The first one exists only when $a^2 \leq m^2$. When $a^2 \neq m^2$, it consists of two disjoint parts,

$$r = r_\pm \stackrel{\text{def}}{=} m \pm \sqrt{m^2 - a^2}. \tag{17.13}$$

As we will see later, it is also a spurious singularity.

It is seen from (17.12) that when $a^2 < m^2$, r becomes time in those regions where $\Delta_r < 0$. Consequently, just as in the Schwarzschild solution, it is impossible to stay at constant r there.

Unlike in the Schwarzschild metric, when $a^2 < m^2$ there exists a region where $\Delta_r > 0$ and $g_{tt} \leq 0$. In it, timelike vectors must have a nonzero φ-component whose minimal value is found from $\mathrm{d}s^2 = 0$ at $\mathrm{d}r = \mathrm{d}\vartheta = 0$ using (17.12):

$$v^\varphi_{\min} = v^0 \frac{2mra - \varepsilon\Sigma\sqrt{\Delta_r}/\sin\vartheta}{2mra^2\sin^2\vartheta + \Sigma\left(r^2 + a^2\right)},$$

where v^0 is the t-component and $\varepsilon \stackrel{\text{def}}{=} a/|a|$. (As expected, $v^\varphi_{\min} \to 0$ when $g_{00} \to 0$, i.e. when $\Sigma \to 2mr$ and $\Delta_r \to a^2\sin^2\vartheta$. The other solution of $\mathrm{d}s^2 = 0$ at $\mathrm{d}r = \mathrm{d}\vartheta = 0$, with $+$ in the numerator, corresponds to the opposite generator of the same light cone and does not have this property.) This is an example of **frame dragging** in the gravitational field of rotating bodies. This effect was first calculated, perturbatively but in a general metric, by Hans Thirring and Josef Lense in 1918 [192]. An experiment to measure it (for a gyroscope orbiting the Earth) was proposed by Leonard Schiff in 1960 [193]. The experiment, under the name of **Gravity Probe B** and under the direction of C. W. Francis Everitt, was carried out in the years 2004 – 2005 [194], after preparations that lasted more than 40 years [195]; see a semi-popular account in Ref. [196].

[192] H. Thirring, *Phys. Zeitschr.* **19**, 33 (1918); **22**, 29 (1921); J. Lense and H. Thirring, *Phys. Zeitschr.* **19**, 156 (1918). Reprinted in B. Mashhoon, F.W. Hehl and D.S. Theiss, *Gen. Relativ. Gravit.* **16**, 711 (1984) and in Ref. [188].

[193] L. Schiff, *Phys. Rev. Lett.* **4**, 215 (1960); *Proc. Nat. Acad. Sci. USA* **46**, 871 (1960).

[194] C. W. F. Everitt et al., *Phys. Rev. Lett.* **106**, 221101 (2011).

[195] C. W. F. Everitt, in Experimental Gravitation. Proceedings of the International School of Physics "Enrico Fermi", course 56. Edited by B Bertotti, Academic Press, New York 1974, p. 331.

[196] https://en.wikipedia.org/wiki/Gravity_Probe_B

The coordinate t in the Schwarzschild metric (and also in (17.12)) coincides with the proper time of an observer at infinity. The ratio of ds of the local observer at rest in the set $g_{tt} = 0$ to the corresponding ds at infinity is zero, which means that the light emitted from $g_{tt} = 0$ arrives to a distant observer with an infinite redshift. Consequently, the set $g_{tt} = 0$ is sometimes called an *infinite redshift hypersurface* by analogy with the Schwarzschild metric.[58] However, as pointed out by Carter [189], this name is misleading. An observer at rest in the B–L coordinates has r, ϑ and φ all constant. On the hypersurface $g_{tt} = 0$ and inside it (where $g_{tt} < 0$), for such an "observer" $\mathrm{d}s^2 \leq 0$, which means that he/she would have to be moving with the velocity of light or faster just to remain at rest relative to infinity. Consequently, stationary observers do not exist where $g_{tt} \leq 0$. This is why a more appropriate name for the set $g_{tt} = 0$ is **the stationary limit hypersurface**.

The existence or nonexistence of regions with $\Delta_r \leq 0$, their geometry and their relation to the regions with $g_{tt} \leq 0$ will be discussed in Sec. 17.3. Their physical meaning will emerge gradually in subsequent sections. For the calculation below we assume that $\Delta_r \geq 0$.

The singularities of the Kerr metric are best recognised when, following Carter [189], the components of the Riemann tensor are projected on the orthonormal basis defined by

$$\begin{aligned} e^0{}_\alpha \mathrm{d}x^\alpha &= \sqrt{\frac{\Delta_r(r)}{\Sigma(r)}}\,\left(\mathrm{d}t - a\sin^2\vartheta \mathrm{d}\varphi\right), \qquad e^1{}_\alpha \mathrm{d}x^\alpha = \sqrt{\frac{\Sigma(r)}{\Delta_r(r)}}\mathrm{d}r, \\ e^2{}_\alpha \mathrm{d}x^\alpha &= \sqrt{\Sigma(r)}\mathrm{d}\vartheta, \qquad e^3{}_\alpha \mathrm{d}x^\alpha = \sin\vartheta\,\frac{a\mathrm{d}t - (r^2+a^2)\,\mathrm{d}\varphi}{\sqrt{\Sigma(r)}}. \end{aligned} \tag{17.14}$$

These projections are

$$\begin{aligned} R_{0101} &= -R_{2323} = 2I_1, \\ R_{0123} &= 2R_{0213} = -2R_{0312} = -2I_2, \\ R_{0202} &= R_{0303} = -R_{1212} = -R_{1313} = -I_1, \\ I_1 &\stackrel{\mathrm{def}}{=} mr\,\frac{r^2 - 3a^2\cos^2\vartheta}{\Sigma^3}, \\ I_2 &\stackrel{\mathrm{def}}{=} ma\cos\vartheta\,\frac{3r^2 - a^2\cos^2\vartheta}{\Sigma^3}. \end{aligned} \tag{17.15}$$

As can be seen, all these components are finite where $\Delta_r = 0$. The singularity is located on the ring $\{r = 0, \vartheta = \pi/2\}$, where $\Sigma = 0$. Since the interior of the ring is nonsingular, one can think of extending the metric through this set, to negative values of r. From (17.6) we see that this is indeed possible, as the (t, x, y, z) coordinates cover both sides of this disc.

Let us note another strange property of the Kerr metric [191, 189]: when ϑ is near $\pi/2$, while r is negative but sufficiently near to zero, then the term $(2mra^2\sin^2\vartheta/\Sigma)$ in the component $g_{\varphi\varphi}$ of (17.12) becomes negative and large in absolute value. Then φ becomes a timelike coordinate and the curves of constant t, ϑ and r in that region are timelike. If we require that, by continuity, these lines are closed with period 2π, then it follows that *closed timelike curves exist in the $r < 0$ sheet of the extended Kerr manifold.* This applies to all three varieties of the Kerr solution ($|a| < m$, $|a| = m$, $|a| > m$; see Sec. 17.3).

[58] But in the Kerr metric, this set *is not* the surface of a black hole, as we will show in Sec. 17.3.

17.3 The event horizons and the stationary limit hypersurfaces.

We have already noted that the hypersurfaces given, in the B–L coordinates, by (17.13), if they exist, play a special role. As we will see later, they are **event horizons**. We also noted that the stationary limit hypersurfaces, given by

$$r^2 - 2mr + a^2\cos^2\vartheta = 0 \Longrightarrow r = m \pm \sqrt{m^2 - a^2\cos^2\vartheta} \tag{17.16}$$

play another special role. We will now consider the shapes of these two families of surfaces and their relation to each other.

When $a^2 < m^2$, there are two event horizons; the one at $r = r_-$ is contained inside that at $r = r_+$. There are also two stationary limit hypersurfaces. The outer one, at $r = m + \sqrt{m^2 - a^2\cos^2\vartheta}$, envelops the outer event horizon, and is tangent to it only at the axis, where $\vartheta = 0$ or $\vartheta = \pi$. The inner stationary limit surface, at $r = m - \sqrt{m^2 - a^2\cos^2\vartheta}$, lies all within the inner event horizon and is tangent to it also only at the axis. It is tangent to the disc $r = 0$ at its singular edge, where it has its own edge. The geometry of these four hypersurfaces is shown in Fig. 17.3.

As $a \to 0$, the Kerr solution tends to the Schwarzschild solution. Then, the inner stationary limit surface and the inner event horizon both shrink to a point, together with the disc $r = 0$. The outer stationary limit surface and the outer event horizon coalesce and go over into the Schwarzschild horizon at $r = 2m$.

As $|a| \to m$, the two event horizons approach each other to meet at $r = m$ when $a^2 = m^2$. The concave regions of the outer stationary limit surface shrink to points, and the surface becomes conical in their neighbourhoods, the vertices of the cones touching the event horizon. Similarly, the inner stationary limit surface becomes conical in the neighbourhood of the axis of symmetry, the vertices of the cones being common with the outer surface. The geometry of these surfaces in the case $a^2 = m^2$ is shown in Fig. 17.4.

When $a^2 > m^2$, the event horizon disappears completely. This case, similarly to the previous one, has no Schwarzschild limit. The conical points of the stationary limit surfaces change to open holes, and the two stationary limit surfaces become parts of one surface that has the topology of a torus. The hole in the surface around the axis of symmetry is the larger, the greater the difference $a^2 - m^2$. The surface still has an edge at $r = 0$, where it is tangent to the disc $r = 0$, but now the "outer" and the "inner" parts of it join smoothly at two rings, given by $(r = m, \vartheta = \arccos(m/a))$ and $(r = m, \vartheta = \pi - \arccos(m/a))$. The geometry of this case is shown in Fig. 17.5.

In the case $a^2 > m^2$ the singular ring at $\{r = 0, \vartheta = \pi/2\}$ becomes accessible: it is a **naked singularity**. The prevailing opinion among astrophysicists is that astronomical objects, when they are about to collapse, must get rid of the excess angular momentum to achieve $a^2 < m^2$ and avoid forming a naked singularity. Nevertheless, the Sun and the Earth have $a^2 > m^2$ (verification of this is an exercise for the reader).

Figure 17.6 shows the 3-dimensional subspace of the Kerr spacetime with $a^2 < m^2$, given by setting $\vartheta = \pi/2$ in (17.12). The vertical axis in the figure is time. The top part of the figure shows a perspective view, the bottom part shows the view from above. The

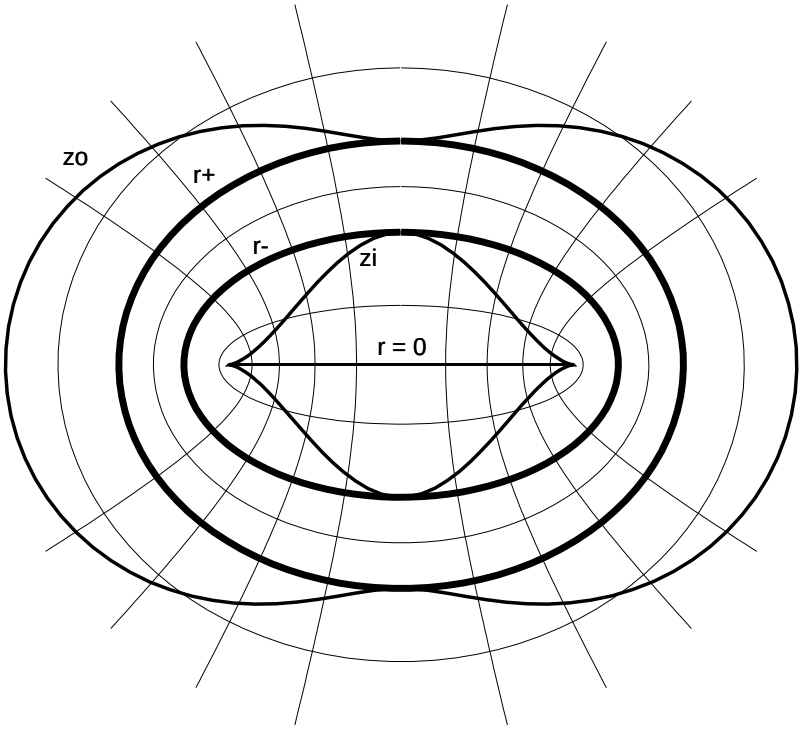

Figure 17.3: Axial cross-section through the space $t =$ constant in the Kerr metric, in the Boyer–Lindquist coordinates, in the case $a^2 < m^2$. The surfaces $r = r_+$ and $r = r_-$ are disjoint, the outer stationary limit surface (z_o in the figure) is tangent to $r = r_+$ at the axis of symmetry. Likewise, the inner stationary limit surface (z_i) is tangent to $r = r_-$ at the axis. The disc $r = 0$ is seen as the horizontal line, the surface z_i has a sharp edge, tangent to the disc. When $|a|/m$ decreases, the surface $r = r_-$ approaches the disc $r = 0$, the surface $r = r_+$ recedes from the disc and becomes more spherical. When $a \to 0$, the disc $r = 0$ and the surfaces z_i and $r = r_-$ all collapse to a single point, while the surfaces z_o and $r = r_+$ coalesce at $r = 2m$ and become spherical.

direction of rotation is clockwise ($a < 0$), so that the X-axis in the top figure would move toward the viewer. The outermost ring is the stationary limit surface at $r = 2m$, the two middle rings are the event horizons $r_\pm$, and the innermost ring is the inner stationary limit surface that, because of $\vartheta = \pi/2$, coincides with the ring singularity at $r = 0$.

Several future light cones are shown. At $r \gg 2m$ they look like slightly deformed Minkowski light cones. At $r = 2m$, one generator of the light cone is parallel to the t-axis: no timelike vector at that point can have a zero φ-component.[59]

As we move from $r = 2m$ towards $r = r_+$, the cones lean forward still further and become thinner in all directions. The limit $r \to r_+$ is discontinuous. As $r \to r_+$ from the $r > r_+$ side, the cones tend to a single beam along the Y-direction in the $T = 0$ plane. The intersections of the cones with a $T =$ constant plane are ellipses that recede to

[59] Because of $g_{t,\varphi} \neq 0$, the time axis is not orthogonal to the $t =$ constant hypersurface, but it is drawn as orthogonal for better readability.

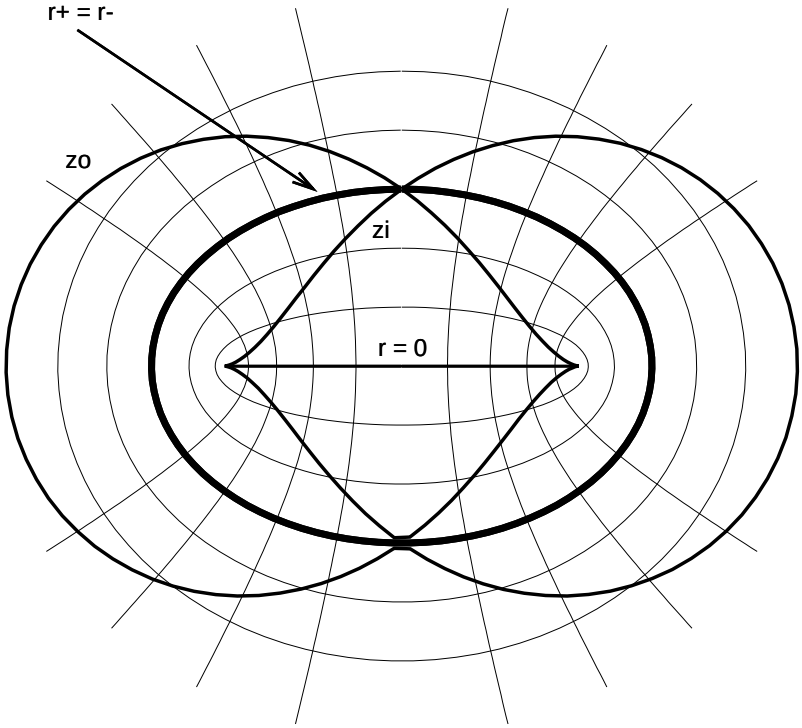

Figure 17.4: Axial cross-section through the space t = constant in the Kerr metric, in the Boyer–Lindquist coordinates, in the case $a^2 = m^2$. There is now a single surface $r = r_+ = r_-$, the surfaces z_o and z_i both touch it at the axis (but are not tangent to it – they approach it at nonzero angle). As $|a| \to m$, the concave areas on the z_o surface from the previous figure shrink to points, and the neighbourhoods of those points becomes conical. The z_i surface becomes conical at the axis as well.

$Y \to -\infty$ as $r \searrow r_+$. As $r \to r_+$ from the $r < r_+$ side, the cones tend to the whole plane $X = \sqrt{{r_+}^2 + a^2}$ = constant (not marked in the figure). The intersections of the cones with the X = constant planes are ellipses elongated and rotated as shown in the inset; their axes both become infinite as $r \nearrow r_+$.

A similar discontinuity exists at $r = r_-$. The intersections of the cones with a T = constant plane again become ellipses in the region $r < r_-$.

Since at $r \nearrow r_+$ the cone degenerates to the plane $X = \sqrt{{r_+}^2 + a^2}$ = constant; no timelike vector attached there can have a zero r-component; in fact r takes over as the time-coordinate here. For $r_- \le r \le r_+$, it is impossible for an ingoing timelike or null curve to turn back without becoming spacelike along an arc or having a nondifferentiable reflection. This shows that $r = r_+$ is an event horizon indeed.

In Fig. 17.6, ingoing and outgoing null curves cross at $r = r_+$, but the B–L coordinates give a false picture here. In reality, there are two event horizons at $r = r_+$. The Kruskal diagram (Fig. 11.9) presents a useful analogy of the situation.[60]

[60] An extension of the Kerr manifold, analogous but not at all similar to that by Kruskal and Szekeres,

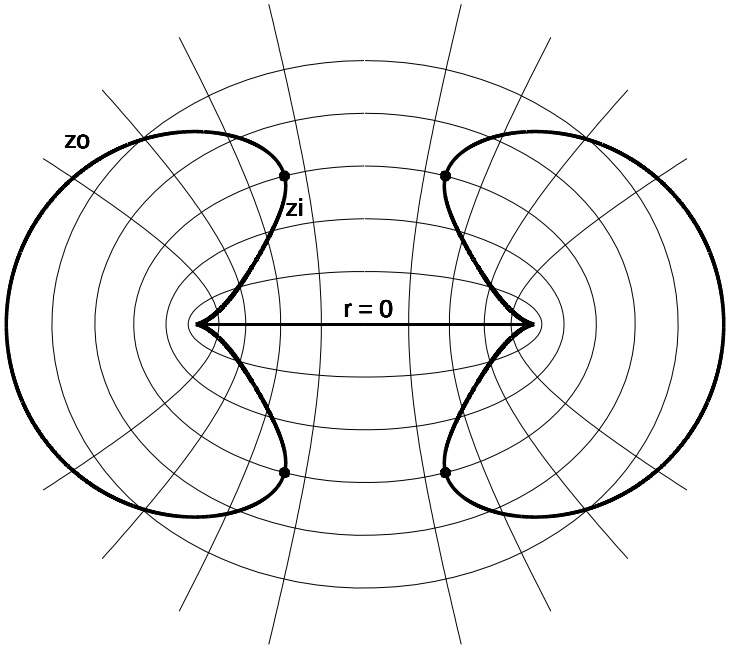

Figure 17.5: An axial cross-section through the space $t =$ constant in the Kerr metric, in the Boyer–Lindquist coordinates, in the case $a^2 > m^2$. The spurious singularities have disappeared, and the two stationary limit surfaces merged into one that has a torus topology. The dots mark the places where z_o (the surface with the +-sign in (17.16)) and z_i meet, this happens at $(r = m, \vartheta = \vartheta_0 \stackrel{\text{def}}{=} \arccos(m/a))$ and $(r = m, \vartheta = \pi - \vartheta_0)$.

At $r < r_-$ the cones are similar to those in the sector $(r_+, 2m)$. As $r \to 0$, they tend to the straight line $\{X = a, T = Y\}$. See Exercise 8 for directions on how to draw Fig. 17.6.

17.4 The Hamiltonian and the Poisson bracket

When looking for an extremum of the functional $\mathcal{L} \stackrel{\text{def}}{=} \int L(q^i(t), \dot{q}^i(t), t)\mathrm{d}t$ (where $\dot{q}^i \stackrel{\text{def}}{=} \mathrm{d}q^i/\mathrm{d}t$) with respect to the functions $q^i(t), i = 1, \ldots, m$, it is often useful to re-express L as a function of $2m$ independent variables q^i and $p_i \stackrel{\text{def}}{=} \partial L/\partial \dot{q}^i$, and then form the Hamiltonian:

$$H \stackrel{\text{def}}{=} \sum_{l=1}^{m} p_l \dot{q}^l(q, p, t) - L. \tag{17.17}$$

was given by Boyer and Lindquist [191]; important preliminary results and generalisations were presented by Carter [197, 198, 189]. See Ref. [11] for the presentation of the Boyer – Lindquist approach.

[197] B. Carter, *Phys. Rev.* **141**, 1242 (1966).
[198] B. Carter, *Phys. Rev.* **174**, 1559 (1968).

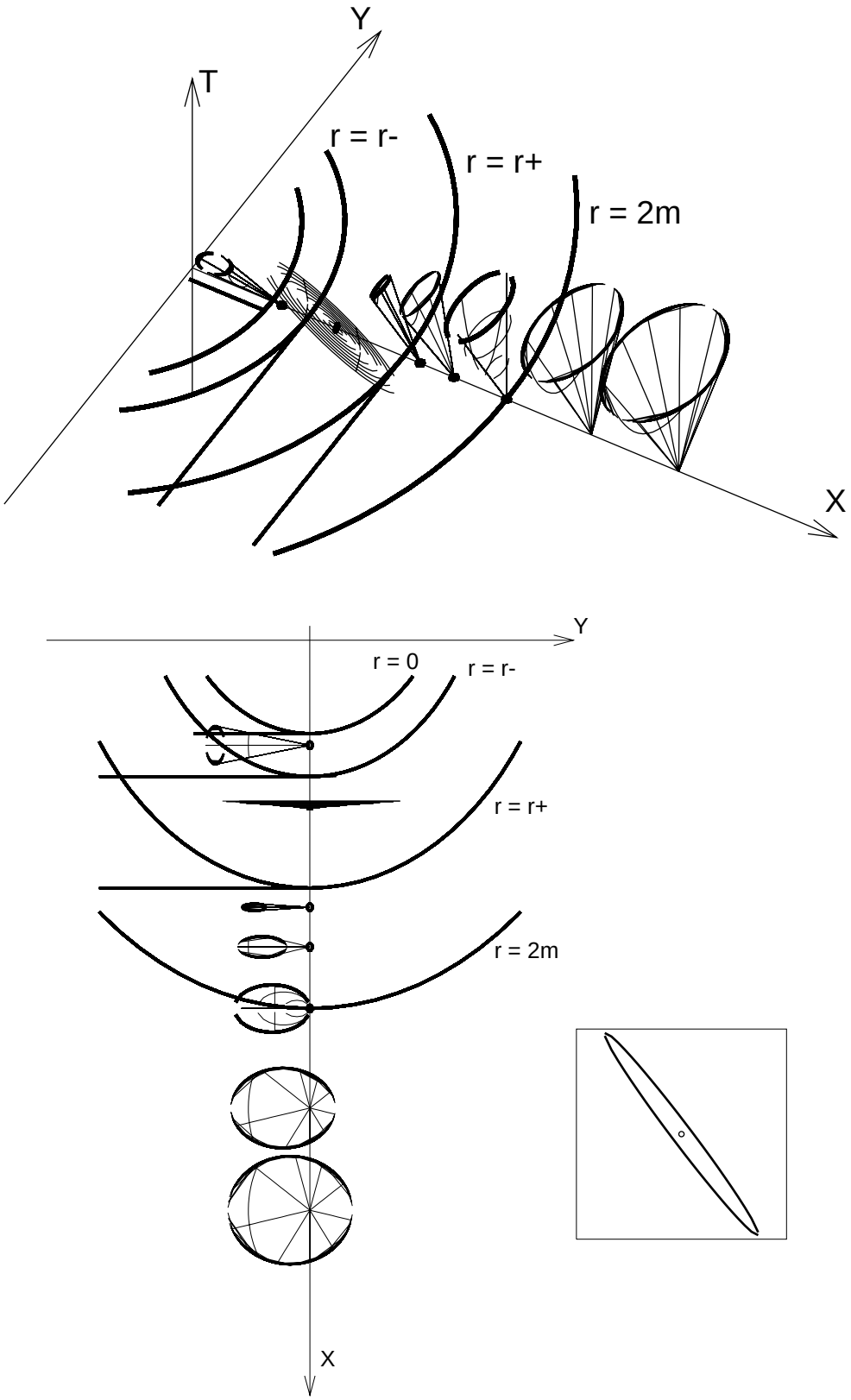

Figure 17.6: A general perspective view (top graph) and a view along the time axis from above (bottom graph) of the Kerr subspace $\vartheta = \pi/2$ in the coordinates of (17.12). Explanation is given in the text. Large dots mark the positions of the vertices of the light cones in the $T = 0$ plane. The inset is an $X =$ constant intersection of the light cone from the sector $r \in (r_-, r_+)$.

The variables q^i and p_i are called positions and momenta, respectively. In terms of H, the Euler – Lagrange equations that determine $q^i(t)$,

$$\frac{\mathrm{d}}{\mathrm{d}t}\left(\frac{\partial L}{\partial \dot{q}^i}\right) - \frac{\partial L}{\partial q^i} = 0,$$

become the Hamilton equations for the functions $q^i(t)$, $p_i(t)$:

$$\dot{q}^i = \frac{\partial H}{\partial p_i}, \qquad \dot{p}_i = -\frac{\partial H}{\partial q^i}. \tag{17.18}$$

This formalism was invented for the needs of mechanics, but is useful for solving the geodesic equations in differential geometry.

The Poisson bracket for the functions $F(q^i, p_i)$ and $G(q^i, p_i), i = 1, \ldots, m$, is defined as

$$\{F, G\} \stackrel{\text{def}}{=} \sum_{l=1}^{m} \left(\frac{\partial F}{\partial q^l}\,\frac{\partial G}{\partial p_l} - \frac{\partial F}{\partial p_l}\,\frac{\partial G}{\partial q^l}\right). \tag{17.19}$$

From the Hamilton equations it follows that for any function $E(q^i, p_i, t)$

$$\frac{\mathrm{d}E}{\mathrm{d}t} = \sum_{l=1}^{m} \left(\frac{\partial E}{\partial q^l}\,\frac{\mathrm{d}q^l}{\mathrm{d}t} + \frac{\partial E}{\partial p_l}\,\frac{\mathrm{d}p_l}{\mathrm{d}t}\right) + \frac{\partial E}{\partial t} = \{E, H\} + \frac{\partial E}{\partial t}. \tag{17.20}$$

So, if E does not depend on t directly (i. e., depends on t only via q^l and p_l) and has zero Poisson bracket with the Hamiltonian, then it is constant along the curve $\{q^i(t), p_i(t)\}$ that obeys the Hamilton equations (17.18).

The Poisson bracket has the following properties:

$$\begin{aligned} \{F, G\} &= -\{G, F\}\,, \qquad \{F_1 + F_2, G\} = \{F_1, G\} + \{F_2, G\}\,, \\ \{F_1 F_2, G\} &= F_1\{F_2, G\} + F_2\{F_1, G\}\,. \end{aligned} \tag{17.21}$$

17.5 General geodesics.

For each Killing field k^α there exists a first integral of the geodesic equations. Let p^α be a vector field tangent to an affinely parametrised geodesic. Then, along the geodesic, $\mathrm{d}(k_\alpha p^\alpha)/\mathrm{d}s = D\left(k_\alpha p^\alpha\right)/\mathrm{d}s = k_{\alpha;\beta} p^\alpha p^\beta + k_\alpha p^\alpha{}_{;\beta}\, p^\beta = 0$, the first term being zero because only $k_{(\alpha;\beta)} = 0$ enters the formula, the second one being zero because p^α is geodesic.

For the Killing fields in the Kerr solution, $\underset{(t)}{k}{}^\alpha = \delta^\alpha_0$ and $\underset{(\varphi)}{k}{}^\alpha = \delta^\alpha_3$, there are two first integrals of the geodesic equations:

$$p_\alpha \underset{(t)}{k}{}^\alpha = p_0 \stackrel{\text{def}}{=} E, \qquad p_\alpha \underset{(\varphi)}{k}{}^\alpha = p_3 \stackrel{\text{def}}{=} -L_z. \tag{17.22}$$

Moreover, there is the first integral $g_{\alpha\beta}p^\alpha p^\beta =$ constant that exists always. For timelike geodesics we choose the affine parameter so that

$$g_{\alpha\beta}p^\alpha p^\beta = {\mu_0}^2, \tag{17.23}$$

where μ_0 is the mass of the orbiting particle. This parametrisation allows for an easy specialisation to null geodesics, for which $\mu_0 = 0$.

For the Kerr metric, there exists a fourth first integral, discovered by Carter [189]. The geodesic equations are the Euler – Lagrange equations for the following Lagrangian:

$$L = \frac{1}{2} g_{\alpha\beta} \frac{\mathrm{d}x^\alpha}{\mathrm{d}s} \frac{\mathrm{d}x^\beta}{\mathrm{d}s} \stackrel{\text{def}}{=} \frac{1}{2} g_{\alpha\beta} \dot{x}^\alpha \dot{x}^\beta . \tag{17.24}$$

The momentum associated to $\dot{x}^\alpha$ is $p_\alpha = g_{\alpha\beta}\dot{x}^\beta$. The corresponding Hamiltonian is

$$H \stackrel{\text{def}}{=} p_\alpha \dot{x}^\alpha - L = \frac{1}{2} g_{\alpha\beta} \dot{x}^\alpha \dot{x}^\beta = L\left(p_\alpha, q^\beta\right). \tag{17.25}$$

The following Lemma holds

Lemma 17.1 *Let the Hamiltonian have the form*

$$H = \frac{1}{2} \frac{H_r + H_\mu}{U_r + U_\mu}, \tag{17.26}$$

where H_μ and U_μ depend only on the coordinate μ, while H_r and U_r depend only on r. The functions H_r and H_μ depend also on p_α, which are independent variables on equal footing with the coordinates, but it is assumed that H_r is independent of the component p_μ and H_μ is independent of the component p_r. Then the quantity

$$K \stackrel{\text{def}}{=} - \frac{U_r H_\mu - U_\mu H_r}{U_r + U_\mu} \tag{17.27}$$

has a vanishing Poisson bracket with the Hamiltonian, and thus is a constant of the motion.

Proof:

By the assumptions made, H_r commutes with H_μ, and obviously H_r commutes with itself. Consequently, for H in the form (17.26), by the rules (17.21), we obtain

$$\begin{aligned} \{H_r, H\} &= \frac{1}{2}\left(H_r + H_\mu\right) \left\{H_r, \frac{1}{U_r + U_\mu}\right\} = \frac{1}{2} \frac{H_r + H_\mu}{\left(U_r + U_\mu\right)^2} \frac{\mathrm{d}U_r}{\mathrm{d}r} \frac{\partial H_r}{\partial p_r} \\ &= \frac{H}{U_r + U_\mu} \{U_r, H_r\} . \end{aligned} \tag{17.28}$$

Since U_r and U_μ do not depend on the momenta, they have zero Poisson brackets among them. So, using the assumptions of the lemma, we have

$$\{U_r, H\} = \frac{1}{2\left(U_r + U_\mu\right)} \{U_r, H_r + H_\mu\} = \frac{1}{2\left(U_r + U_\mu\right)} \frac{\mathrm{d}U_r}{\mathrm{d}r} \frac{\partial H_r}{\partial p_r} = \frac{1}{2\left(U_r + U_\mu\right)} \{U_r, H_r\} . \tag{17.29}$$

From (17.29) and (17.28) we see that

$$\{H_r, H\} = 2H \{U_r, H\} . \tag{17.30}$$

Now it is easy to verify that

$$K \stackrel{\text{def}}{=} 2U_r H - H_r \equiv \frac{U_r H_\mu - U_\mu H_r}{U_r + U_\mu} \tag{17.31}$$

commutes with H, and so is a constant of the motion. $\square$

For applying the Hamilton method to the geodesic equations in the Kerr metric, it is convenient to rewrite the metric in the form equivalent to (17.12):

$$\mathrm{d}s^2 = \frac{\Delta_r}{\Sigma}\left[\mathrm{d}t - a\left(1-\mu^2\right)\mathrm{d}\varphi\right]^2 - \frac{1-\mu^2}{\Sigma}\left[a\mathrm{d}t - \left(r^2+a^2\right)\mathrm{d}\varphi\right]^2 - \Sigma\left(\frac{\mathrm{d}r^2}{\Delta_r} + \frac{\mathrm{d}\mu^2}{1-\mu^2}\right), \tag{17.32}$$

where Σ and Δ_r were defined in (17.7) and (17.11), respectively, and

$$\mu \stackrel{\text{def}}{=} \cos\vartheta. \tag{17.33}$$

The Lagrangian and the Hamiltonian are found from (17.25) using (17.32):

$$H = L = \frac{1}{2}\left\{\frac{\Delta_r}{\Sigma}\left[\dot{t} - a\left(1-\mu^2\right)\dot{\varphi}\right]^2 - \frac{1-\mu^2}{\Sigma}\left[a\dot{t} - \left(r^2+a^2\right)\dot{\varphi}\right]^2 - \Sigma\left(\frac{\dot{r}^2}{\Delta_r} + \frac{\dot{\mu}^2}{1-\mu^2}\right)\right\}. \tag{17.34}$$

From here we find the momenta using the definition $p_i \stackrel{\text{def}}{=} \partial L/\partial\dot{q}^i$:

$$p_t = \left(1 - \frac{2mr}{\Sigma}\right)\dot{t} + \frac{2mra\sin^2\vartheta}{\Sigma}\dot{\varphi}, \tag{17.35}$$

$$p_\varphi = \frac{2mra\sin^2\vartheta}{\Sigma}\dot{t} - \left(\frac{2mra^2\sin^2\vartheta}{\Sigma} + r^2 + a^2\right)\sin^2\vartheta\dot{\varphi}, \tag{17.36}$$

$$p_r = -\frac{\Sigma}{\Delta_r}\,\dot{r}, \qquad p_\mu = -\frac{\Sigma}{1-\mu^2}\,\dot{\mu}. \tag{17.37}$$

Now it can be verified that the Hamiltonian (17.34) rewritten in terms of the momenta (17.35) – (17.37), with terms grouped as in (17.26), is equivalent to

$$H = \frac{-\Delta_\mu {p_\mu}^2 - {\Delta_\mu}^{-1}\left(a\Delta_\mu p_t + p_\varphi\right)^2}{2\Sigma} + \frac{-\Delta_r {p_r}^2 + {\Delta_r}^{-1}\left[\left(r^2+a^2\right)p_t + ap_\varphi\right]^2}{2\Sigma}, \tag{17.38}$$

where $\Delta_\mu \stackrel{\text{def}}{=} 1-\mu^2 \equiv \sin^2\vartheta$, and $\Sigma \equiv r^2 + a^2\mu^2$.

Comparing (17.38) with (17.26) we identify the parts of the Hamiltonian as follows:

$$H_r = -\Delta_r {p_r}^2 + {\Delta_r}^{-1}\left[\left(r^2+a^2\right)p_t + ap_\varphi\right]^2, \tag{17.39}$$

$$H_\mu = -\Delta_\mu {p_\mu}^2 - {\Delta_\mu}^{-1}\left(a\Delta_\mu p_t + p_\varphi\right)^2, \tag{17.40}$$

$$U_r = r^2 + a^2, \qquad U_\mu = -a^2\left(1-\mu^2\right) \equiv -a^2\sin^2\vartheta \tag{17.41}$$

(the splitting of Σ into U_r and U_μ was done so that it agrees with Carter's notation [189]). Using the above in (17.27) we obtain for the fourth constant of the motion

$$K = \frac{\left(r^2+a^2\right)\left\{\Delta_\mu {p_\mu}^2 + \Delta_\mu^{-1}\left[a\Delta_\mu p_t + p_\varphi\right]^2\right\}}{\Sigma}$$

$$+ \quad \frac{a^2\Delta_\mu \left\{ \Delta_r {p_r}^2 - \Delta_r^{-1} \left[\left(r^2+a^2\right) p_t + a p_\varphi \right]^2 \right\}}{\Sigma} \tag{17.42}$$

$$= \quad a^2 \sin^2\vartheta \left[\frac{\Sigma}{\Delta_r}\, \dot{r}^2 - \frac{\Delta_r}{\Sigma} \left(a\sin^2\vartheta\dot{\varphi} - \dot{t} \right)^2 \right]$$

$$+ \quad \left(r^2+a^2\right) \left\{ \Sigma\dot{\vartheta}^2 + \frac{\sin^2\vartheta}{\Sigma} \left[\left(r^2+a^2\right)\dot{\varphi} - a\dot{t} \right]^2 \right\}. \tag{17.43}$$

The constants defined in (17.22) and (17.23) are

$$E = \frac{r^2 - 2mr + a^2\cos^2\vartheta}{\Sigma}\, \dot{t} + \frac{2mra\sin^2\vartheta}{\Sigma}\, \dot{\varphi}, \tag{17.44}$$

$$L_z = -\frac{2mra\sin^2\vartheta}{\Sigma}\, \dot{t} + \frac{\left[-\Delta_r a^2 \sin^2\vartheta + \left(r^2+a^2\right)^2 \right] \sin^2\vartheta}{\Sigma}\, \dot{\varphi}, \tag{17.45}$$

$${\mu_0}^2 = -\Sigma \left(\frac{\dot{r}^2}{\Delta_r} + \dot{\vartheta}^2 \right) - \frac{\sin^2\vartheta}{\Sigma} \left[\left(r^2+a^2\right)\dot{\varphi} - a\dot{t} \right]^2 + \frac{\Delta_r}{\Sigma} \left(a\sin^2\vartheta\dot{\varphi} - \dot{t} \right)^2. \tag{17.46}$$

These equations can now be solved for the velocities, which allows for some general discussion. We introduce the following new functions

$$R(r) \stackrel{\text{def}}{=} -K\Delta_r - {\mu_0}^2 \left(r^2+a^2\right)\Delta_r + \left[\left(r^2+a^2\right)E - aL_z \right]^2, \tag{17.47}$$

$$\Theta(\vartheta) \stackrel{\text{def}}{=} K + {\mu_0}^2 a^2 \sin^2\vartheta - \sin^2\vartheta \left(aE - \frac{L_z}{\sin^2\vartheta} \right)^2. \tag{17.48}$$

The components of the velocity are then given by

$$\Sigma^2\dot{r}^2 = R(r), \tag{17.49}$$

$$\Sigma^2\dot{\vartheta}^2 = \Theta(\vartheta), \tag{17.50}$$

$$\Sigma\dot{\varphi} = \left(\frac{1}{\sin^2\vartheta} - \frac{a^2}{\Delta_r} \right) L_z + \frac{2mra}{\Delta_r}\, E, \tag{17.51}$$

$$\Sigma\dot{t} = -\frac{2mra}{\Delta_r}\, L_z + \left[\frac{\left(r^2+a^2\right)^2}{\Delta_r} - a^2\sin^2\vartheta \right] E. \tag{17.52}$$

This can be disentangled still further. From (17.49) – (17.50) we see that $\Sigma\dot{\vartheta}/\sqrt{\Theta(\vartheta)} = \Sigma\dot{r}/\sqrt{R(r)} = 1$. We take the quotient of these two equations to obtain (17.53), and their sum to obtain (17.54) below. In deriving (17.54) we substitute for Σ and group the terms so that each integrand depends on just one coordinate. The result is

$$\int \frac{\mathrm{d}\vartheta}{\sqrt{\Theta}} = \int \frac{\mathrm{d}r}{\sqrt{R}} = Q = \text{constant}, \tag{17.53}$$

$$\lambda - \lambda_0 = \int \frac{a^2\cos^2\vartheta \mathrm{d}\vartheta}{\sqrt{\Theta}} + \int \frac{r^2\mathrm{d}r}{\sqrt{R}}, \tag{17.54}$$

where λ is the affine parameter. These equations implicitly determine $r(\lambda)$ and $\vartheta(\lambda)$.

In order to disentangle (17.51) – (17.52) in a similar way, we note from (17.49) – (17.50) that $1/\Sigma = \dot{\vartheta}/\sqrt{\Theta(\vartheta)} = \dot{r}/\sqrt{R(r)}$, and use one or the other of these equations to obtain an integrand that is a function of r only, or one that is a function of ϑ only. The result is

$$\varphi - \varphi_0 = \int \frac{L_z \mathrm{d}\vartheta}{\sin^2\vartheta\sqrt{\Theta}} + \int \frac{2mraE - a^2 L_z}{\Delta_r \sqrt{R}}\, \mathrm{d}r, \tag{17.55}$$

$$t - t_0 = \int \frac{\left(r^2+a^2\right)^2 E - 2mraL_z}{\Delta_r\sqrt{R}}\, \mathrm{d}r - \int \frac{a^2 \sin^2\vartheta E}{\sqrt{\Theta}}\, \mathrm{d}\vartheta. \tag{17.56}$$

In this form, the geodesic equations can be solved and investigated numerically. The equations of null geodesics follow as the subcase $\mu_0 = 0$.

Without numerical integration, only a few qualitative conclusions may be drawn. For example, if an orbit lies in the equatorial plane ($\vartheta = \pi/2$ and $\dot{\vartheta} = 0$ on the whole orbit) or is tangent to that plane at one point ($\vartheta = \pi/2$ and $\dot{\vartheta} = 0$ only at that point), then

$$C \stackrel{\mathrm{def}}{=} K + {\mu_0}^2 a^2 - (aE - L_z)^2 = 0. \tag{17.57}$$

For the orbits that cross the equatorial plane at nonzero angle, $C > 0$ (because $R \geq 0$ and $\Theta \geq 0$ from (17.49) – (17.50)). For the orbits that never go through $\vartheta = \pi/2$, C may be negative. For the orbits that run along the symmetry axis, $L_z = 0$.

Equation (17.57) being fulfilled all along a geodesic is a necessary and sufficient condition for it to lie in an equatorial plane. The necessity was shown above, for the sufficiency see Exercise 9.

A detailed investigation of timelike geodesics in the Kerr solution, also in its generalisation for Λ, was carried out by Kraniotis [199] – [203]. The author continues the series.

17.6 Geodesics in the equatorial plane.

This section is based on the papers by Bardeen [204] and by Boyer and Lindquist [191].

In a spherically symmetric spacetime, each timelike or null geodesic lies in a plane, and then the coordinate axes can be chosen so that it is the equatorial plane. In the Kerr spacetime we do not have that freedom. The equatorial plane in the BL coordinates is

[199] G. V. Kraniotis, Precise relativistic orbits in Kerr and Kerr-(anti) de Sitter spacetimes. *Class. Quant. Grav.* **21**, 4743 (2004).

[200] G. V. Kraniotis, Frame dragging and bending of Light in Kerr and Kerr-(anti) de Sitter spacetimes. *Class. Quant. Grav.* **22**, 4391 (2005).

[201] G. V. Kraniotis, Periapsis and gravitomagnetic precessions of stellar orbits in Kerr and Kerr-de Sitter black hole spacetimes. *Class. Quant. Grav.* **24**, 1775 (2007).

[202] G. V. Kraniotis, Precise analytic treatment of Kerr and Kerr-(anti) de Sitter black holes as gravitational lenses. *Class. Quant. Grav.* **28**,085021 (2011).

[203] G. V. Kraniotis, Gravitational lensing and frame dragging of light in the Kerr-Newman and the Kerr-Newman-(anti) de Sitter black hole spacetimes. *Gen. Relativ. Gravit.* **46**, 1818 (2014).

[204] J. M. Bardeen, in: *Black holes – les astres occlus.* Edited by C. de Witt and B. S. de Witt. Gordon and Breach, New York, London, Paris 1973, p. 219.

$\vartheta = \pi/2$, and a given geodesic either lies in it or does not. Equations (17.49) – (17.56) simplify a lot when it does, and we will consider this case now.

Consider (17.49) with $\vartheta = \pi/2$, $\dot{\vartheta} = 0$. The motion can take place where $R(r) \geq 0$. Let us treat $R(r)$ as a function of E. For motions in the equatorial plane, $C = 0$ in (17.57). Substituting in (17.47) for K found from (17.57) with $C = 0$ we get

$$\frac{1}{r}\, R(r) = \left[r\left(r^2 + a^2\right) + 2ma^2\right] E^2 - 4amL_z E - (r - 2m){L_z}^2 - r\Delta_r {\mu_0}^2. \tag{17.58}$$

The discriminant of R/r as a function of E is

$$\delta = 4r\Delta_r \left\{r{L_z}^2 + {\mu_0}^2\left[r\left(r^2 + a^2\right) + 2ma^2\right]\right\}, \tag{17.59}$$

and for $r > 0$ the signs of δ and Δ_r are the same. Hence, $R(r)$ has zeros only in those regions where $\Delta_r \geq 0$. Note also that $p^0 > 0$: since $p^0 \propto \mathrm{d}x^0/\mathrm{d}s$, the opposite would mean that the particle moves backward in time. From (17.22) and (17.12) we find

$$p^0 = g^{00}E + g^{03}L_z = \frac{B}{\Delta_r \Sigma}\ (E - \omega L_z), \tag{17.60}$$

where

$$B \stackrel{\text{def}}{=} \left(r^2 + a^2\right)^2 - \Delta_r a^2 \sin^2\vartheta \geq 0, \qquad \omega \stackrel{\text{def}}{=} 2amr/B. \tag{17.61}$$

Hence, $p^0 > 0 \Longleftrightarrow E > \omega L_z$, which, in the plane $\vartheta = \pi/2$, reduces to

$$E > \frac{2am}{D}\ L_z. \tag{17.62}$$

The two roots of the equation $R(r) = 0$ are

$$E_\pm = \frac{1}{D}\ \left[2amL_z \pm \sqrt{\Delta_r\left(r^2{L_z}^2 + {\mu_0}^2 rD\right)}\right], \qquad D \stackrel{\text{def}}{=} r\left(r^2 + a^2\right) + 2ma^2, \tag{17.63}$$

but E_- does not obey (17.62). Thus, the motion can only occur where $E > E_+$.

If $a^2 < m^2$, then $\Delta_r > 0$ for $r < r_-$ and for $r > r_+$, where $r_\pm$ are given by (17.13). For $r_- < r < r_+$, $\delta < 0$ in (17.59), so $R(r) \neq 0$ there, and thus $\mathrm{d}r/\mathrm{d}s \neq 0$. Hence, there exist no circular orbits and no turning points in that region. A freely falling body that enters the region (r_-, r_+) from the side of $r > r_+$ must fly all through it to the hypersurface $r = r_-$. However, it does not have to hit the singularity, since the orbit can have a turning point at $r < r_-$. Conversely, a body that entered the region (r_-, r_+) from the side of $r < r_-$ must fly all through it to the hypersurface $r = r_+$.

More information about the orbits follows from the graph of $E_{\min}(r) = E_+(r)$; see Fig. 17.7. We consider only the case $a^2 < m^2$ and the region $r > r_+$, so the curves begin at $r = r_+$. Each orbit has a constant $E \geq E_{\min}(r)$. Thus, the area accessible for motion is above the graph of $E_{\min}(r)$, and the value of E determines the allowed range of r on the orbit. Note that $E_{\min}/\mu_0 \underset{r\to\infty}{\longrightarrow} 1$, independently of the value of L_z.

When $L_z = 0$, $\mathrm{d}(E_{\min}/\mu_0)/\mathrm{d}r > 0$ for all $r \geq r_+$, so $E_{\min}/\mu_0 < 1$ for all $r \geq r_+$. However, if $|L_z|$ is sufficiently large, then there exists an interval (r_1, r_2) (where $r_+ \leq r_1 < r_2$) in

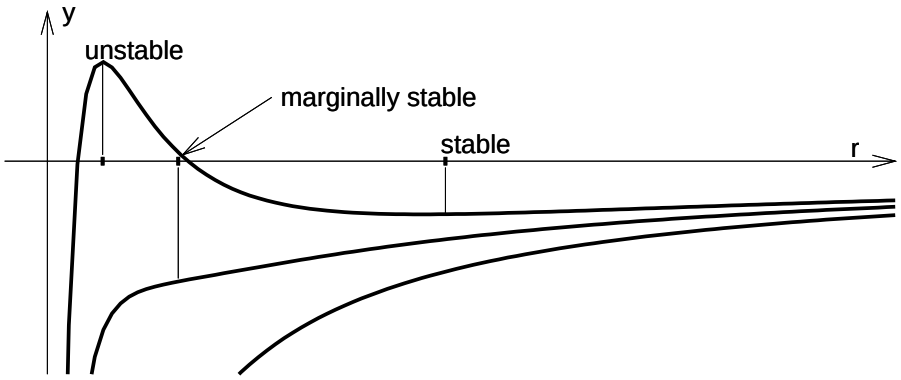

Figure 17.7: Graphs of the function $y(r) \stackrel{\text{def}}{=} E_{\min}(r)/\mu_0 - 1$ for different values of L_z. For every value of L_z, $y(r) \to 0$ as $r \to \infty$. The lower graph corresponds to $L_z = 0$, then $y(r)$ is all monotonic. The upper graph corresponds to $|L_z|$ being large, $y(r)$ then has a maximum that determines the position of the unstable circular orbit, and a minimum that determines the stable circular orbit. The middle graph approximately corresponds to such L_z, at which the maximum and the minimum coalesce into a single point where $\mathrm{d}^2y/\mathrm{d}r^2 = 0$. This point determines the radius of the marginally stable circular orbit. The curves begin at $r = r_+$; the y-axis is drawn approximately there.

which $E_{\min}/\mu_0 \geq 1$, while for $r > r_2$ $E_{\min}/\mu_0 < 1$ (see Exercise 4), independently of the sign of L_z. Thus, with $|L_z|$ sufficiently large, $E_{\min}/\mu_0$ necessarily has a local maximum at some $r = r_u > r_+$ and a local minimum at $r = r_s > r_u$, just as is shown in Fig. 17.7. The region where $E_{\min}/\mu_0 < 1$ is the locus of bound orbits, and $r = r_s$ is the radius of the stable circular orbit (i.e. there exists one for each sufficiently large value of $|L_z|$, for each sign of L_z). A circular orbit also exists at $r = r_u$, but it is unstable.

The parameter L_z is the orbital angular momentum of the body on the geodesic, while a is the angular momentum per unit mass of the source of the gravitational field. When $aL_z > 0$, the two angular momenta are parallel, such orbits are called **direct**. When $aL_z < 0$, they are antiparallel, such orbits are called **retrograde**. The value of $E_{\min}$ in (17.63) at a given r is different for each of these orbits. This difference is a relativistic effect: in Newton's theory the two types of orbits are the same.

The difference between them in relativity is quite pronounced. Note from (17.63) that with $aL_z < 0$ and r sufficiently close to r_+ (i.e. with Δ_r close to zero) $E_{\min} < 0$, so E can be negative. If $E > 0$, then it is the rest energy of the particle "at infinity".[61] Thus, $E < 0$ means that the whole energy contained in the particle is insufficient to actually move it to infinity. This effect does not appear for $aL_z > 0$, or in the Schwarzschild limit $a = 0$.

Where can negative-energy orbits exist? To verify, let us take the Kerr metric in the BL coordinates, (17.12), then let us choose at each point of the spacetime the following orthonormal vector basis $e^i{}_\alpha$ (in which $g^{\alpha\beta}e^i{}_\alpha e^j{}_\beta = g^{ij} = \mathrm{diag}(+1,-1,-1,-1)$):

$$e^0{}_\alpha \mathrm{d}x^\alpha = \mathrm{e}^\nu \mathrm{d}t, \qquad e^1{}_\alpha \mathrm{d}x^\alpha = \mathrm{e}^\lambda \mathrm{d}r, \qquad e^2{}_\alpha \mathrm{d}x^\alpha = \sqrt{\Sigma}\mathrm{d}\vartheta, \qquad e^3{}_\alpha \mathrm{d}x^\alpha = \mathrm{e}^\psi(\mathrm{d}\varphi - \omega \mathrm{d}t), \tag{17.64}$$

[61] "At infinity" special relativity applies, so $p^0 = E$ is the energy of the particle at rest.

where B and ω were defined in (17.61),[62] and

$$\mathrm{e}^{2\nu} = \frac{\Delta_r \Sigma}{B}, \qquad \mathrm{e}^{2\lambda} = \frac{\Sigma}{\Delta_r}, \qquad \mathrm{e}^{2\psi} = \frac{B}{\Sigma}\sin^2\vartheta. \tag{17.65}$$

The projections of the momentum defined in (17.22) on $e_{\hat{0}}{}^{\alpha}$ and $e_{\hat{3}}{}^{\alpha}$ are then

$$p_{\hat{0}} = \mathrm{e}^{-\nu}\left(E - \omega L_z\right), \qquad p_{\hat{3}} = \mathrm{e}^{-\psi} p_3 = -\mathrm{e}^{-\psi} L_z. \tag{17.66}$$

In consequence of $p^0 > 0$ and (17.60), $p_{\hat{0}} = p^{\hat{0}} > 0$ where $\Delta_r > 0$. The p_i obey

$$p_{\hat{0}}{}^2 - p_{\hat{1}}{}^2 - p_{\hat{2}}{}^2 - p_{\hat{3}}{}^2 = {\mu_0}^2 > 0 \Longrightarrow |p_{\hat{3}}| < p_{\hat{0}}. \tag{17.67}$$

From (17.66), $E = \mathrm{e}^{\nu} p_{\hat{0}} - \omega \mathrm{e}^{\psi} p_{\hat{3}}$. Hence, $E < 0 \Longrightarrow \omega p_{\hat{3}} > 0$ (this is consistent with $aL_z < 0$ since all quantities in ω other than a are positive.) So, using (17.67), $E < 0$ implies $\mathrm{e}^{\nu} p_{\hat{0}} < \mathrm{e}^{\psi}|\omega|\,|p_{\hat{3}}| < \mathrm{e}^{\psi}|\omega| p_{\hat{0}}$. It follows that $\omega^2 \mathrm{e}^{2\psi} > \mathrm{e}^{2\nu}$, which means $g_{00} < 0$. Thus, orbits with negative energy can exist only between the stationary limit hypersurfaces.

This was a necessary condition for the existence of orbits with $E < 0$. What is a sufficient condition? Suppose $p_{\hat{1}} = 0$ at the initial point. Then $p_{\hat{0}}$ is bounded because $p_{\hat{0}}{}^2 = {\mu_0}^2 + p_{\hat{2}}{}^2 + p_{\hat{3}}{}^2$, while $p_{\hat{2}}{}^2 = \Sigma^2 \dot{\vartheta}^2$ and $p_{\hat{3}}{}^2 = \mathrm{e}^{-2\psi} {L_z}^2$ are both bounded in the region $\{r > r_+,\ \sin\vartheta \neq 0\}$; see (17.50) and (17.61).[63] Consequently, $\mathrm{e}^{\nu} p_{\hat{0}}$ can be made as small as we wish by taking r sufficiently close to r_+. Then, since $E = \mathrm{e}^{\nu} p_{\hat{0}} + \omega L_z$, and $\omega \neq 0$ at $r \geq r_+$, it is enough to take $aL_z < 0$ and such r that $\mathrm{e}^{\nu} p_{\hat{0}} < |\omega L_z|$ to achieve $E < 0$.

Equation (17.63) simplifies for photon orbits, for which $\mu_0 = 0$:

$$E^{\nu}_{\min} = |L_z| \, \frac{r\sqrt{\Delta_r} \pm 2am}{D}, \tag{17.68}$$

where "+" corresponds to $L_z > 0$, and "−" to $L_z < 0$. For any sign, the function $F(r) \stackrel{\text{def}}{=} E^{\nu}_{\min} / |L_z|$ has only one maximum and no minima for $r \in (r_+, \infty)$ (see Exercise 5). Thus, where $\Delta_r > 0$, a photon orbit in the equatorial plane can have only one turning point and there are no stable circular orbits. For any L_z, there exists a circular orbit that lies on the maximum of $F(r)$, and so is unstable. The same is true in the Schwarzschild limit $a = 0$ [52]. A representative graph of the function $F(r)$ is shown in Fig. 17.8.

As seen from (17.49) and (17.58), if $\mu_0 = 0$ and the affine parameter is redefined by $s = Es'$, then E and L_z are present only in the combination L_z/E. Consequently, $E = 1$ may be assumed without loss of generality. We redefine some of the variables as follows:

$$\rho \stackrel{\text{def}}{=} r/(2m), \qquad \lambda \stackrel{\text{def}}{=} -L_z/(2m), \qquad \alpha \stackrel{\text{def}}{=} = a/(2m). \tag{17.69}$$

Then we get from (17.49) and (17.58)

$$\dot{r}^2 = \frac{1}{\rho^3}\left[\rho^3 + \left(\alpha^2 - \lambda^2\right)\rho + (\alpha + \lambda)^2\right] \stackrel{\text{def}}{=} \frac{1}{\rho^3}\,\psi(\rho). \tag{17.70}$$

[62] To verify that (17.64) leads to (17.12) show that $\Delta_r \Sigma^2 - 4a^2 m^2 r^2 \sin^2\vartheta = B\left(r^2 - 2mr + a^2\cos^2\vartheta\right)$.

[63] The assumption $p_{\hat{1}} = 0$ was necessary because ${p_{\hat{1}}}^2 \propto \dot{r}^2/\Delta_r$ and is not bounded when $\Delta_r \to 0$.

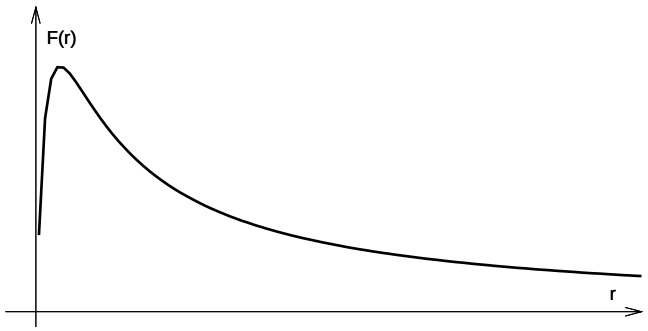

Figure 17.8: The analogue of Fig. 17.7 for null geodesics in the equatorial plane. The curve begins at $r = r_+$. The graph has the same general shape for all values of L_z.

The turning points of the null geodesics are at the zeros of $\psi(\rho)$, and the motion can take place in those ranges of ρ where $\psi(\rho)/\rho^3 > 0$. Since the Kerr manifold can be extended to include also negative values of r [191, 11], we will take them into account here.

Apart from the special case $\alpha = -\lambda$ (i.e. $a = L_z$), $\psi(0) > 0$, while $\psi < 0$ for sufficiently large $-\rho > 0$. Thus, ψ typically has a real root at $\rho = \rho_1 < 0$ and is positive for some $\rho > \rho_1$. So, any ray sent in from $r = -\infty$ will eventually return to $r = -\infty$ (the ray with $\alpha = -\lambda$ hits the singularity at $r = 0$). If $\lambda^2 \leq \alpha^2$ while $\lambda \neq -\alpha$, then there are no positive roots of ψ, and any ray coming from $\rho > 0$ will hit the singularity. If λ^2 is smaller than some ${\lambda_1}^2$, then $\psi > 0$ for all $\rho > 0$ and such rays will hit the singularity, too. However, if λ^2 is sufficiently large, then ψ will have two positive roots. In that case, there will be rays that come in from $r = +\infty$ and turn back at a $\rho_2 > 0$, possibly after circling the central body several times, and rays that come from the side of $r = 0$ and turn back toward $r = 0$ after reaching a maximal distance $0 < \rho_1 < \rho_2$. The situation is shown in Fig. 17.9. Figs. 17.10 and 17.11 show the situation when $a^2 = m^2$ and $a^2 > m^2$, respectively. The contours separating the allowed and prohibited areas are graphs of the $\lambda(\rho)$ function found by solving the equation $\psi(\rho) = 0$ for λ; from the definition (17.70), the solution is

$$\lambda = \frac{-\alpha \pm |\rho|\sqrt{\rho^2 - \rho + \alpha^2}}{1 - \rho} \stackrel{\text{def}}{=} \lambda_\pm(\rho). \tag{17.71}$$

The relation between the various branches of $\lambda(\rho)$ depends on the sign of ρ, in consequence of $|\rho|$ in front of the square root in (17.71). Namely, in the $\rho < 0$ area of Fig. 17.9, the upper branch corresponds to $\lambda_-(\rho)$, and the lower branch to $\lambda_+(\rho)$, while the opposite is true where $\rho > 0$. Note that it is ψ/ρ^3 that must be positive in the allowed region, hence in the $\rho < 0$ area the allowed region is where $\psi < 0$.

For timelike geodesics, a similar analysis can be carried out, but more subcases have to be considered. This time we can choose the affine parameter so that $\mu_0 = 1$. We define $\Gamma \stackrel{\text{def}}{=} E^2 - 1$, and, using (17.69), we obtain from (17.49) and (17.58) (with $\vartheta = \pi/2$):

$$\dot{r}^2 = \frac{1}{\rho^3}\left[\Gamma\rho^3 + \rho^2 + \left(\alpha^2\Gamma - \lambda^2\right)\rho + (\alpha E + \lambda)^2\right] \stackrel{\text{def}}{=} \frac{1}{\rho^3}\,\overline{\psi}(\rho). \tag{17.72}$$

The allowed range of r is given by $\overline{\psi}(\rho)/\rho^3 \geq 0$. The zeros of $\overline{\psi}(\rho)$ exist only for those

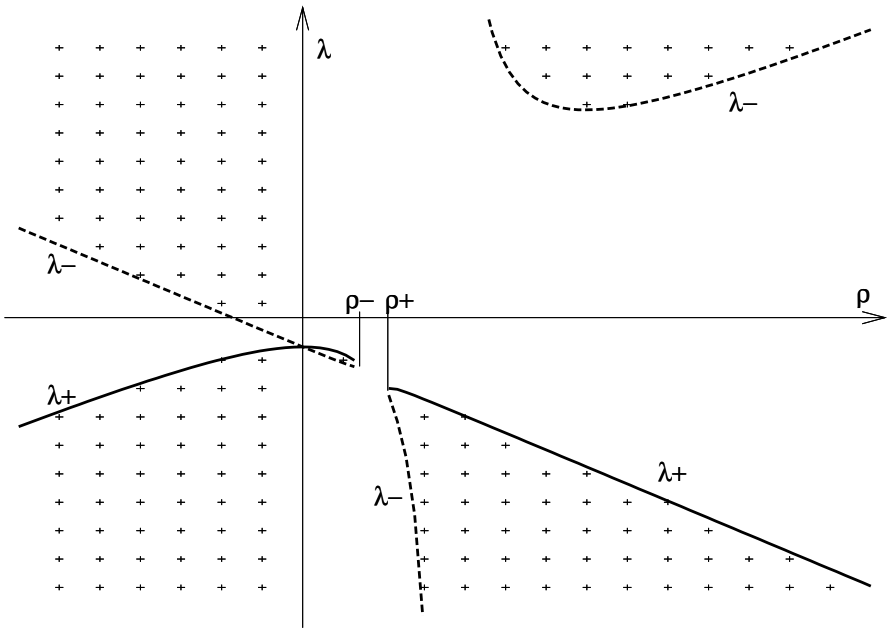

Figure 17.9: The allowed ranges of λ and ρ for null geodesics in the case $a^2 < m^2$ (the areas covered with crosses are prohibited). For λ sufficiently small or sufficiently large, the rays can either emanate from $\rho = 0$ and turn back at a finite distance, or come in from $r = +\infty$ and turn back to infinity at a finite distance. In between, on the $\rho > 0$ side, the rays mostly hit $\rho = 0$, except for a small range of λ, in which there is the little prohibited "peninsula". On the $\rho < 0$ side, all rays that come in from the direction of $r = -\infty$ turn back at a finite distance, except the rays with $\lambda = -\alpha$ that hit the singularity. The right tip of the peninsula is at $\rho = \rho_-$, the radius of the inner event horizon. The left tip of the prohibited wedge in the $\rho > 0$ region is at $\rho = \rho_+$, the outer event horizon. With decreasing α, the peninsula shrinks and its left tip moves toward the ρ-axis (and so does the tip of the white wedge on the left), the upper prohibited area on the right moves down and left, while the lower prohibited area moves down and right. In the limit $a = 0$ the peninsula disappears, and the whole graph becomes mirror-symmetric with respect to the ρ-axis. For what happens when a increases, see Figs. 17.10 and 17.11.

values of ρ at which the discriminant of $\overline{\psi}(\rho)$ treated as a function of λ is non-negative:

$$\delta = 4\rho\,(\rho - \rho_-)\,(\rho - \rho_+)\,(\Gamma\rho + 1) \geq 0, \tag{17.73}$$

where $\rho_\pm$ are the coordinates of the event horizons; $\rho_- < 1/2$, $\rho_- < \rho_+ < 1$. Note that $\Gamma \geq -1$ by definition. The following cases have to be considered

Case 1: $\Gamma < 0$.

Then $|\Gamma| \leq 1$, and $\delta \geq 0$ for $0 \leq \rho \leq \rho_-$ and for $\rho_+ \leq \rho \leq 1/|\Gamma|$. By considering the signs of δ and of $(1 - \rho)$ (the coefficient of λ^2), the following cases are discerned:

a) $\rho < 0$ – this area is all prohibited;

b) $0 \leq \rho \leq \rho_-$ – orbits exist for $\lambda \leq \lambda_-$ and for $\lambda \geq \lambda_+$, where

$$\lambda_\pm(\rho) = \frac{1}{1-\rho}\,\left(-\alpha E \pm \sqrt{\delta}\right); \tag{17.74}$$

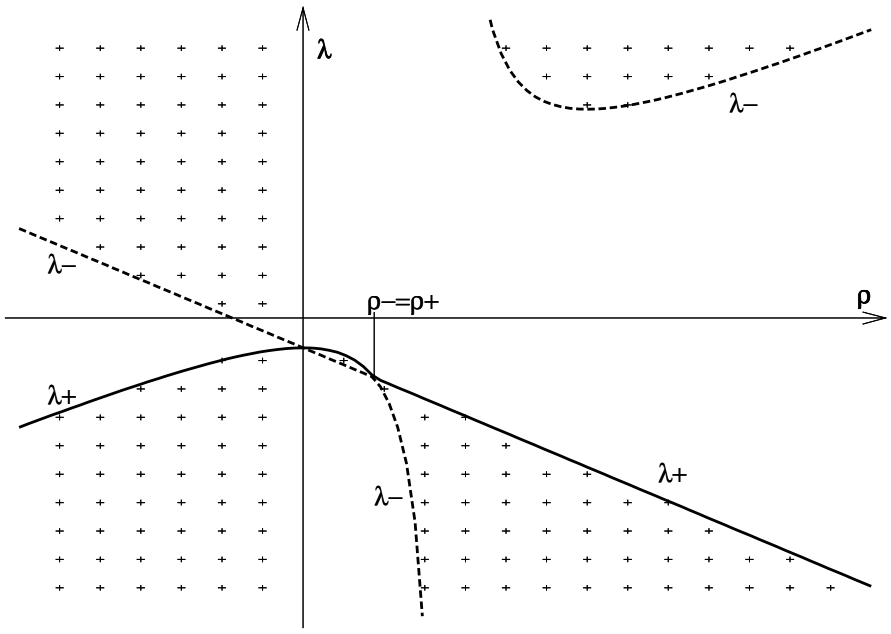

Figure 17.10: The allowed ranges of λ and ρ for null geodesics in the critical case $a^2 = m^2$. The little prohibited peninsula from Fig. 17.9 has extended to touch the tip of the lower prohibited area. The contact point has $\rho = \rho_- = \rho_+$; the ρ-coordinate of the single remaining horizon.

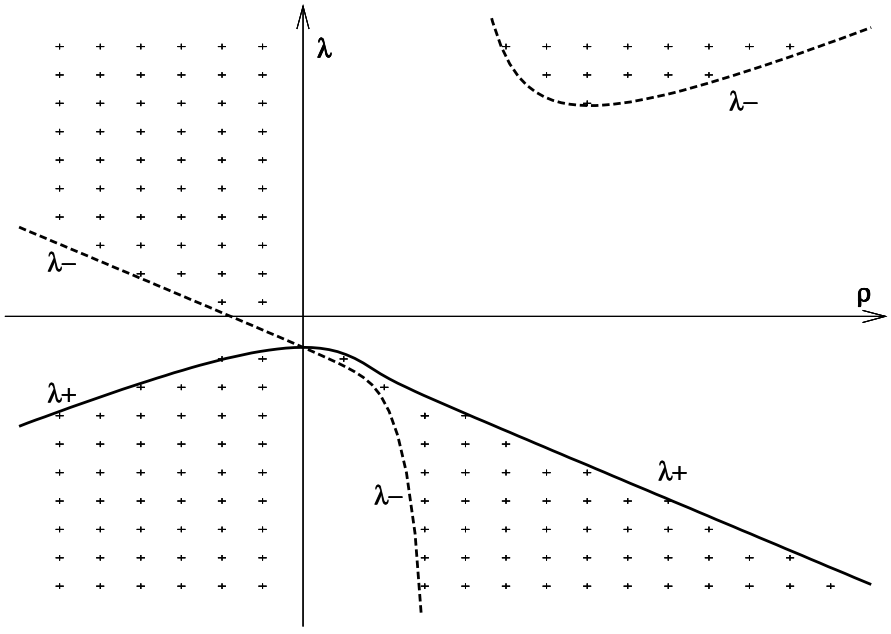

Figure 17.11: The allowed ranges of λ and ρ for null geodesics in the case $a^2 > m^2$. The two prohibited areas at $\{\rho > 0, \lambda < 0\}$ merged into one. As a^2 increases, the lower prohibited wedge becomes gradually wider and its tip moves down, while the upper prohibited area on the right moves up and farther to the right.

(note that $\lambda_- < \lambda_+$ when $\rho < 1$ and $\lambda_+ < \lambda_-$ when $\rho > 1$);

c) $\rho_- < \rho < \rho_+$ – all values of λ are allowed;

(d) $\rho_+ \leq \rho < 1$ – orbits exist for $\lambda \leq \lambda_-$ and for $\lambda \geq \lambda_+$;

(e) $\rho = 1$ – orbits exits for $\lambda \geq -\left[\Gamma\left(2\alpha^2+1\right)+\alpha^2+1\right]/(2\alpha E)$;

(f) $1 < \rho \leq 1/|\Gamma|$ – orbits exist for $\lambda_+ \leq \lambda \leq \lambda_-$;

(g) $\rho > 1/|\Gamma|$ – this area is all prohibited.

Fig. 17.12 shows Case 1 with $a > 0$. The curves $\lambda(\rho)$ determined by $\overline{\psi}(\rho) = 0$ have vertical tangents at $\rho = 0$, $\rho = \rho_\pm$, $\rho \to 1$ and at $\rho = -1/\Gamma$. At $\rho > 1$, the part above each "belly" in the main figure is the $\lambda_-(\rho)$ branch, the part below is $\lambda_+(\rho)$. At $\rho < 1$, the roles of λ_- and λ_+ reverse, with λ_- going to $+\infty$ or $-\infty$ as $\rho \to 1^\pm$, respectively. Curve (a) corresponds to $\Gamma = -1$, curves (b) – (d) correspond to increasing values of Γ. On curve (a) necessarily $\rho \leq 1$, and the allowed range of λ is above and below the curve. The other curves run in the $\rho > 1$ sector, in which the allowed range is between λ_- and λ_+. This can be briefly summarised by saying that the allowed area is to the left of each curve. The inset shows a magnified view of the region $0 \leq \rho \leq \rho_-$, where small prohibited "peninsulas", similar to the one seen in Fig. 17.9, exist.

Case 2: $\Gamma > 0$

Then $\delta \geq 0$ and there are the following ranges of ρ to consider: (a) $\rho \leq -1/\Gamma$, (b) $-1/\Gamma < \rho < 0$, (c) $0 \leq \rho \leq \rho_-$, (d) $\rho_- < \rho < \rho_+$, (e) $\rho_+ \leq \rho \leq 1$, (f) $\rho > 1$.

In cases (a), (c) and (e) the allowed range is $\lambda \leq \lambda_-$ and $\lambda \geq \lambda_+$, in case (f) the allowed range $\lambda_- \leq \lambda \leq \lambda_+$, in the remaining two cases all values of λ are allowed.

Case 3: $\Gamma = 0$.

Details of Case 2 and the whole Case 3 are left as an exercise for the readers.

Bound orbits exist in those cases where a line $\lambda =$ constant in the graph has a segment that runs in the allowed region and has both ends on the same $\lambda(\rho)$ curve. In Fig. 17.12 such bound states exist for curves (c) and (d), two of them are shown.

17.7 The Penrose process.

Penrose [205] contemplated a process by which, *in principle*, the rotational energy of a Kerr black hole can be extracted. The idea is based on the observation we made after eq. (17.67), that a body on a retrograde orbit inside the outer stationary limit hypersurface (OSLH) can have a negative energy if it is close enough to the event horizon $r = r_+$. In brief, Penrose's idea was this: put two masses at the ends of a spring, then squeeze the spring and bind the masses together. Then send the composite on an orbit that enters the

[205] R. Penrose, in *Riv. Nuovo Cimento, Numero Speziale* **I**, 252 (1969); reprinted in *Gen. Relativ. Gravit.* **34**, 1141 (2002), with an editorial note by A. Królak, *Gen. Relativ. Gravit.* **34**, 1135 (2002) and author's biography by W. Israel, *Gen. Relativ. Gravit.* **34**, 1138 (2002).

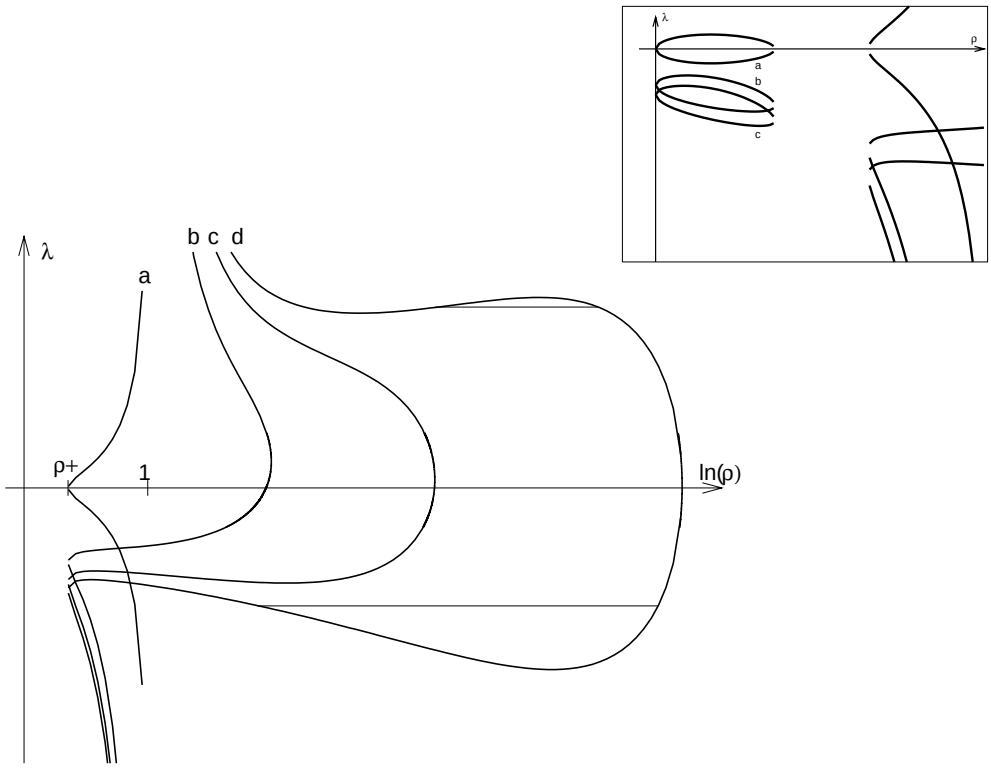

Figure 17.12: The allowed ranges of λ and ρ for timelike geodesics in the case $a^2 < m^2$, for different values of Γ. All the curves correspond to $a > 0$ and $\Gamma < 0$; Γ increases from curve (a) (on which $\Gamma = -1 \iff E = 0$) to curve (d). The allowed areas are to the left of each curve. With $\Gamma < 0$, the whole region $\rho < 0$ is prohibited. Little prohibited peninsulas similar to the one from Fig. 17.9 are present also here, they are shown in the inset (where curve (d) is omitted). The scale on the ρ-axis is logarithmic in the main figure and linear in the inset. Horizontal lines show the allowed ranges of ρ on two bound orbits. Since $a > 0$ for all curves, $\lambda > 0$ corresponds to retrograde orbits, and $\lambda < 0$ to direct orbits; the figure clearly shows their inequivalence. There exist allowed regions also with $\rho < 0$ when $\Gamma > 0$, see the text.

region between the OSLH and $r = r_+$, called **ergosphere**.[64] Design the orbit so that it has its turning point close to $r = r_+$ (how close will become clear below). When the composite object is at the turning point, release the spring in such a direction that one of the masses is sent, with initial $\dot{r} = 0$, on a retrograde orbit with $E < 0$ and with $|L_z|$ sufficiently small for it to fall through the event horizon. It follows from the reasoning between eqs. (17.66) and (17.68) that this is possible: we direct the ejected mass so that $aL_z < 0$, we make $|L_z|$ small enough that the mass is sure to go through $r = r_+$ (see Fig. 17.12), and the orbit has to be pre-designed so that at the turning point $\mathrm{e}^{\nu} p_{\hat{0}} < |\omega L_z|$.

Since the mass dropped into the black hole carried away some negative energy, the other mass acquires some additional energy and additional momentum by recoil. Consequently, it will return to the outside of the OSLH having a greater energy than it had at the beginning of the journey. This trick can be applied for as long as the OSLH exists. The

[64] The name comes from the Greek word $\varepsilon\rho\gamma o$, meaning "work" – because, as shown below, a rotating black hole is in principle able to do some work by extracting energy from the ergosphere.

logical conclusion is that the extra energy carried away by the returning mass was gained at the expense of the rotational energy of the black hole: the slower the b. h. rotates, the smaller $|a|$ becomes, and the smaller the volume of the ergosphere. However, this is a speculation that goes beyond the area of applicability of the Kerr metric. In order to discuss this energy extraction process in a correct way, we would have to use a nonstationary solution in which the angular momentum of the rotating body can depend on time.

17.8 Stationary-axisymmetric spacetimes and locally non-rotating observers.

A spacetime is **stationary** when it has a timelike Killing field $\underset{(0)}{k}{}^{\alpha}$ (if $\underset{(0)}{k}{}^{\alpha}$ is hypersurface-orthogonal, then the spacetime is **static**). It is **axisymmetric** when it has a Killing field $\underset{(3)}{k}{}^{\alpha}$ whose integral lines are closed.[65] For **stationary-axisymmetric spacetimes** it is assumed in addition that the two Killing fields commute. (The Kerr metric is an example: the length of the lines of constant (t, r, ϑ) in (17.12) is zero at $\vartheta = 0$.) Then, coordinates can be chosen so that the metric is independent of $x^0 = t$ (where $\mathrm{d}x^\alpha/\mathrm{d}t = \underset{(0)}{k}{}^{\alpha}$) and of $x^3 = \varphi$ (where $\mathrm{d}x^\alpha/\mathrm{d}\varphi = \underset{(3)}{k}{}^{\alpha}$). Let the other two coordinates be x^1 and x^2.

It is also assumed that the surfaces generated by the Killing fields admit orthogonal surfaces, i.e. that in the coordinates adapted to the Killing fields $g_{01} = g_{02} = g_{13} = g_{23} = 0$ (this property is called **orthogonal transitivity**). In these coordinates the metric, and the motion of matter if any is present, is invariant under the discrete transformation $(t, \varphi) \to (-t, -\varphi)$.[66] Several theorems were proven in which $[\, \underset{(0)}{k}, \underset{(3)}{k}\,] = 0$ and orthogonal transitivity follow from other assumptions (see Ref. [33] for a brief listing). Their intention was to show that spacetimes that do not possess these properties are rare or unimportant or weird. The fact is, though, that not much is known about the cases left out.

In a stationary-axisymmetric spacetime that is orthogonally transitive, coordinates in the (x^1, x^2) surfaces can be chosen so that $g_{12} = 0$ [11]. The metric is thus:

$$\mathrm{d}s^2 = g_{00}\mathrm{d}t^2 + 2g_{03}\mathrm{d}t\mathrm{d}\varphi + g_{33}\mathrm{d}\varphi^2 + g_{11}\mathrm{d}(x^1)^2 + g_{22}\mathrm{d}(x^2)^2. \qquad (17.75)$$

When nothing else is assumed about the two Killing fields, the basis of their space can be chosen arbitrarily. The transformation of the basis

$$\underset{(0)}{k}{}' = C_0 \underset{(0)}{k} + D_0 \underset{(3)}{k}, \qquad \underset{(3)}{k}{}' = C_3 \underset{(0)}{k} + D_3 \underset{(3)}{k}$$

[65] It is often demanded in addition that there exists a location in the spacetime at which the length of the integral lines of $\underset{(3)}{k}{}^{\alpha}$ goes to zero. This is excessive because, even in two dimensions, there exist axially symmetric surfaces that do not contain such a location, for example cylinders and one-sheeted hyperboloids.

[66] An example of a configuration that does not obey this is a rotating gaseous body, inside which the gas circulates in the meridional planes.

induces a transformation of the adapted coordinates; the (t', φ') adapted to $\underset{(0)}{k}{}'$ and $\underset{(3)}{k}{}'$ are

$$t' = C_0 t + C_3 \varphi, \qquad \varphi' = D_0 t + D_3 \varphi. \tag{17.76}$$

The transformed $g_{\alpha\beta}$ is still independent of t and φ, and is orthogonally transitive, only g_{00}, g_{03} and g_{33} are reshuffled among themselves. However, the Killing fields $\underset{(0)}{k}{}^{\alpha}$ and $\underset{(3)}{k}{}^{\alpha}$ are *unique* if the spacetime is asymptotically flat. Then, at infinity the integral lines of $\underset{(3)}{k}$ are closed, and φ is periodic with period 2π. This excludes those transformations (17.76) in which $C_3 \neq 0$, or else the strange behaviour illustrated in Fig. 17.13 would occur: after increasing φ by $2\pi C_3 D_0 / (C_0 D_3 - C_3 D_0)$ we would land at the same t'-line from which we started, but with the t' coordinate increased by $\Delta t' \stackrel{\text{def}}{=} -2\pi C_3$. The orbits of the $\underset{(3)}{k}$ field would thus be changed into infinite helices, while on two sides of the initial t'-line adjacent points would exist whose time-coordinate would differ by $\Delta t'$. The t' coordinate would thus fail to be a continuous function of the spacetime point.[67]

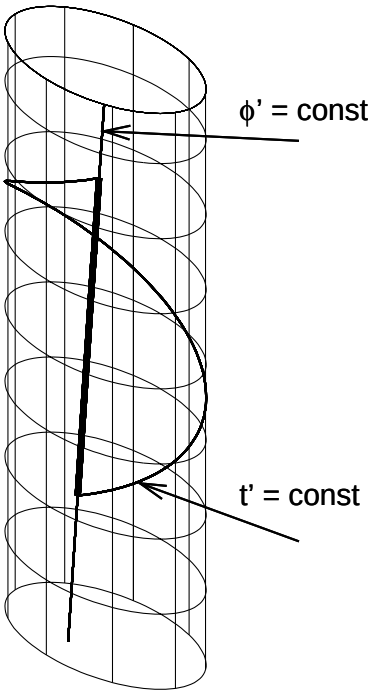

Figure 17.13: A coordinate transformation of the form (17.76) would result in disrupting the orbits of the $\underset{(3)}{k}$ field and in a discontinuous time coordinate. The thick helix segment shows the jump in t' along the $\varphi' = 0$ line, equal to $\Delta t'$ given in the text.

The constant D_0 has to be zero for a different reason. Suppose the coordinates of the asymptotically flat spacetime go over, at infinity, into the cylindrical coordinates in which

$$\mathrm{d}s^2 = \mathrm{d}t^2 - r^2 \mathrm{d}\varphi^2 - \mathrm{d}r^2 - \mathrm{d}z^2. \tag{17.77}$$

[67] However, exactly this kind of time coordinate is used on the surface of the Earth – the discontinuity occurs across the line of change of date that runs through the middle of the Pacific.

This means that asymptotically g_{03} and g_{33}/r^2 must go to zero and to -1, respectively. After a transformation (17.76) with $D_0 \neq 0$, the g_{03} component would become

$$g'_{03} = \frac{1}{D_3 C_0}\left(g_{03} - \frac{D_0}{D_3} g_{33}\right),$$

and would be nonzero at infinity. So, $D_0 = 0$ in consequence of asymptotic flatness.

Finally, $D_3 = 1$ in order that the period of φ is 2π. Thus, the only remaining freedom is the choice of the unit of time, connected with the constant C_0.

Because of this uniqueness, *locally nonrotating observers* [206] exist. Write (17.75) as

$$\mathrm{d}s^2 = \mathrm{e}^{2\nu}\mathrm{d}t^2 - \mathrm{e}^{2\psi}\left(\mathrm{d}\varphi - \omega \mathrm{d}t\right)^2 - \mathrm{e}^{2\lambda}\mathrm{d}r^2 - \mathrm{e}^{2\mu}\mathrm{d}\vartheta^2. \tag{17.78}$$

Now imagine an observer moving with the four-velocity U^α such that $U^r = U^\vartheta = 0$, i.e. circulating within the (t, φ) surface. Define $\Omega \stackrel{\mathrm{def}}{=} U^\varphi/U^t \equiv \mathrm{d}\varphi/\mathrm{d}t$ – this is the angular velocity of the observer. Imagine that she has set up mirrors all along her orbit so that light rays sent by her can travel around the same circle in both directions and come back to her. Let the time of the round-trip of the light ray be T_ε, with $\varepsilon = +1$ for the ray rotating forward, and $\varepsilon = -1$ for the ray rotating backward with respect to the observer. The observer will during the time T_ε move from the position φ_1 to the position $\varphi_2 = \varphi_1 + \Omega T_\varepsilon$. The light ray, during its round trip, will move from φ_1 to $\varphi_3 = \varphi_1 + \Omega T_\varepsilon + 2\pi\varepsilon$. Along the ray $\mathrm{d}s^2 = 0$, so $\varepsilon \mathrm{e}^\nu \mathrm{d}t = \mathrm{e}^\psi(\mathrm{d}\varphi - \omega \mathrm{d}t)$, and consequently

$$\mathrm{d}t = \frac{1}{\omega + \varepsilon \mathrm{e}^{\nu-\psi}}\,\mathrm{d}\varphi. \tag{17.79}$$

Integrating this over the whole round-trip we get

$$T_\varepsilon = \frac{\Omega T_\varepsilon + 2\pi\varepsilon}{\omega + \varepsilon \mathrm{e}^{\nu-\psi}}. \tag{17.80}$$

Solving this for T_ε we obtain

$$T_\varepsilon = \frac{2\pi}{\mathrm{e}^{\nu-\psi} - \varepsilon(\Omega - \omega)}. \tag{17.81}$$

Along the observer's path $\mathrm{d}\varphi = \Omega \mathrm{d}t$, so her proper time s is related to t by

$$\mathrm{d}s^2 = \left[\mathrm{e}^{2\nu} - \mathrm{e}^{2\psi}(\Omega - \omega)^2\right]\mathrm{d}t^2. \tag{17.82}$$

Hence, the proper time of the round-trip of the ray measured by the observer is

$$S_\varepsilon = \sqrt{\mathrm{e}^{2\nu} - \mathrm{e}^{2\psi}(\Omega - \omega)^2}\,T_\varepsilon \equiv 2\pi \mathrm{e}^\psi \sqrt{\frac{1 + \varepsilon \mathrm{e}^{\psi-\nu}(\Omega - \omega)}{1 - \varepsilon \mathrm{e}^{\psi-\nu}(\Omega - \omega)}}. \tag{17.83}$$

This time is different for the forward ray and for the backward ray ($S_1 \neq S_{-1}$) except when $\Omega = \omega$. Since, as has been shown, in an asymptotically flat spacetime the (t, φ) coordinates of (17.78) are unique, ω is uniquely determined by the geometry, and so *there is a uniquely determined set of observers for whom the effect of rotation,* $(S_1 - S_{-1})$, *disappears.* They

[206] J. M. Bardeen, *Astrophys. J.* **162**, 71 (1970).

are called **locally nonrotating observers** [206]. Their worldlines are orthogonal to the $t =$ constant hypersurfaces, and so the rotation tensor defined by (12.31) is zero.

The quantities present in (17.78) were defined for the Kerr metric in eqs. (17.61) and (17.65). The Kerr metric is stationary, axisymmetric and asymptotically flat, with the period of φ equal to 2π, so it allows the existence of locally nonrotating observers.

17.9 A source of the Kerr field?

The Kerr solution has been known for more than 50 years now, and from the beginning it provoked the question: what material body could generate such a vacuum field around it? Several authors tried to find a model of the source, but so far without success. The most promising result is that of Roos [207]. He investigated the existence of perfect fluid sources for stationary axisymmetric vacuum metrics. In application to the Kerr metric, he proved that the Einstein equations in the source are integrable in a finite neighbourhood of the hypersurface given by $r = r_0\left(1 + \sin^2\vartheta\right)$ (where $r_0 > r_+$) in the BL coordinates, but there exist no solutions if the boundary hypersurface is $r = r_0 =$ constant.

All the attempts to find a reasonable explicit solution failed so far [208].[68] The sources known are all rather artificial (see Ref. [208] for references): a 2-dimensional disc spanned on the singular ring of the Kerr metric, a body with anisotropic stresses, sometimes enveloped in a crust of another kind of anisotropic matter. The continuing lack of success prompted some authors to suggest that a perfect fluid source might not exist. The opinion of this author is that a bright new idea is needed, as opposed to routine standard tricks tested so far. It is enough to have a look at the Newtonian models of rotating bodies that, even in the apparently simple cases of homogeneous density distribution, are really tricky [209] to realise that the corresponding problem in relativity must be at least as difficult.

17.10 Exercises

1. Prove that the Schwarzschild solution has the property (17.1).

Note: This is an invariant property, and it does not matter which coordinates you choose.

2. Prove that the vector field l_μ in (17.1) is null with respect to $g_{\mu\nu}$ if and only if it is null with respect to $\eta_{\mu\nu}$. Prove then that $l^\mu \stackrel{\text{def}}{=} g^{\mu\nu}l_\nu \equiv \eta^{\mu\nu}l_\nu$ and verify that (17.2) holds.

3. Verify that if x, y and z are Cartesian coordinates, then the surfaces $r =$ constant defined by (17.8) are confocal ellipsoids of revolution. Since they are axially symmetric,

[207] W. Roos, *Gen. Relativ. Gravit.* **7**, 431 (1976).

[208] A. Krasiński, *Ann. Phys.* **112**, 22 (1978).

[68] Ref. [208] contains a systematic overview of the attempts prior to 1976; all the later attempts can be classified according to that same scheme and none moved the matter forward.

[209] S. Chandrasekhar, *Ellipsoidal figures of equilibrium.* Yale University Press, New Haven and London 1969, p. 46.

the foci of cross-sections through the axis all lie on a circle. Verify that the radius of that circle is equal to a and that $2r$ is the smallest diameter of the ellipsoid $r = \text{constant}$.

4. Prove that with $a^2 < m^2$ and a sufficiently large $|L_z|$, there exists a range (r_1, r_2), with $r_+ \le r_1 < r_2$, such that $E_{\min}(r)/\mu_0 > 1$ for $r_1 < r < r_2$ and $E_{\min}(r)/\mu_0 < 1$ for $r > r_2$.

Hint: Substitute (17.63) in the inequality $E_{\min}(r)/\mu_0 > 1$ and simplify. Note that $r^2\Delta_r - 4a^2m^2 = (r-2m)D$. If ${L_z}^2$ is large enough, then the discriminant of the resulting square trinomial in r is positive, hence $E_{\min}(r)/\mu_0 > 1$ for $r_1 < r < r_2$, with

$$r_{1,2} = \frac{1}{4m}\left[\left(\frac{L_z}{\mu_0}\right)^2 \mp \sqrt{\left(\frac{L_z}{\mu_0}\right)^4 - 16m^2\left(\frac{L_z}{\mu_0} - a\right)^2}\right],$$

and $E_{\min}(r)/\mu_0 < 1$ for $r > r_2$. Then verify that $r_1 \ge r_+$ for any L_z.

5. Prove that the function $F(r) \stackrel{\text{def}}{=} E^{\nu}_{\min}/\,|L_z|$ defined in (17.68) has only one maximum and no minima in the range $r \in (r_+, \infty)$.

Hint: 1. Note that $F = (r-2m)/\left(r\sqrt{\Delta_r} \mp 2am\right)$ and that $F \neq 0$ at $r = 2m$ with the lower sign because the denominator vanishes there, too, and the limit of the whole expression is finite. This remark applies also to the derivatives of F. 2. Calculate $\mathrm{d}F/\mathrm{d}r$ and observe that it is $+\infty$ at $r = r_+$ and goes to zero from below as $r \to \infty$, hence has at least one zero in the range $r \in (r_+, \infty)$. 3. The equation $\mathrm{d}F/\mathrm{d}r = 0$ has the form $\sqrt{\Delta_r}+$ (polynomial in r) $= 0$. Solve this for $\sqrt{\Delta_r}$ and square the result. The resulting 5-th degree equation factorises and becomes $(r-2m)^2\left(r^3 - 6mr^2 + 9m^2r - 4ma^2\right) \stackrel{\text{def}}{=} (r-2m)^2H(r) = 0$. (The $r = 2m$ is not a zero of $\mathrm{d}F/\mathrm{d}r$: with the $-$-sign, the limit of $F'(r)$ at $r \to 2m$ is finite; with the $+$-sign, $F'(r)$ has a nonzero value there.) 4. Observe that $H(r)$ has two zeros in the range $r \in (r_+, \infty)$, but only one of them is also a zero of $F'(r)$. This is done as follows: $H(r)$ is positive at $r = r_+$ and at $r = 4m$, but negative at its minimum at $r = 3m$. Thus one of its zeros is in $(r_+, 3m)$ and the other in $(3m, 4m)$. Now, with the $-$-sign, $F'(r)$ changes sign an odd number of times in $(r_+, 3m)$, but an even number of times in $(3m, 4m)$, hence the second zero of H is not a zero of F'. With the $+$-sign, the opposite is true: $F'(r)$ changes sign an even number of times in $(r_+, 3m)$, but an odd number of times in $(3m, 4m)$, so the first zero of H is not a zero of F'. Consequently, F' has only one zero in (r_+, ∞). That this corresponds to a maximum of F follows from point 2 above: F is increasing in the neighbourhood of $r = r_+$ and decreasing as $r \to \infty$.

6. Draw graphs analogous to Fig. 17.12 for the cases $\Gamma > 0$ and $\Gamma = 0$ (preferably by using a good plotting program).

7. Prove that for the locally nonrotating observers of sec. 17.8, the rotation tensor is zero and the worldlines of these observers are orthogonal to the $r = \text{constant}$ hypersurfaces.

8. Find the equations of the light cones in Fig. 17.6.

Hint: The metric of the subspace $\vartheta = \pi/2$ in (17.12) is

$$\mathrm{d}s^2 = \left(1 - \frac{2m}{r}\right)\mathrm{d}t^2 + \frac{4ma}{r}\,\mathrm{d}t\mathrm{d}\varphi - \left(\frac{2ma^2}{r} + r^2 + a^2\right)\mathrm{d}\varphi^2 - \frac{r^2}{\Delta_r}\,\mathrm{d}r^2.$$

The equation of the light cones is $\mathrm{d}s^2 = 0$. The relation between the B–L coordinates (r, φ) and the (X, Y) spatial coordinates in the figure is $X = \sqrt{r^2 + a^2}\cos\varphi$, $Y = \sqrt{r^2 + a^2}\sin\varphi$. The cones are drawn at the points of the plane $\varphi = 0$, where $\mathrm{d}r = \left(\sqrt{r^2 + a^2}/r\right)\mathrm{d}X$, $\mathrm{d}\varphi = \mathrm{d}Y/\sqrt{r^2 + a^2}$. Thus the equation of a cone with vertex at $(T, X, Y) = (0, 0, X_0)$ is

$$\left(1 - \frac{2m}{r}\right)T^2 + \frac{4ma}{r\sqrt{r^2 + a^2}}\,TY - \left[\frac{2ma^2}{r\,(r^2 + a^2)} + 1\right]Y^2 - \frac{r^2 + a^2}{\Delta_r}\,(X - X_0)^2 = 0.$$

The vertical axis in the figure is T, the (X, Y) axes are as shown. The equations for drawing the graphs are obtained by solving the above for T or for X, but a few special cases must be treated separately. The limit $r = 2m$ (the outer stationary limit hypersurface) in the above equation is nonsingular. Before taking the limits $r \to r_\pm$, the equation must be multiplied by Δ_r. These limits are discontinuous, as described at the end of Sec. 17.3. On approaching $r = r_\pm$ from inside the segment (r_-, r_+), the equation becomes $X = X_0(r_\pm)$, which is a vertical plane. On approaching these values from outside of that segment, the equation becomes singular, but by calculating the curves along which the cones intersect with a $T =$ constant plane one finds that they are ellipses whose both axes shrink to a point, while the ellipses themselves recede to $Y \to -\infty$ as $r \to r_\pm$. Before taking the limit $r \to 0$, the equation must be multiplied by r; in the limit it becomes $-2m\,[T - (a/|a|)Y]^2 = 0$, which is one of the straight lines $T = Y$ (when $a > 0$) or $T = -Y$ (when $a < 0$, the case shown in the figure).

9. Show that if (17.57) is fulfilled all along a geodesic, then the geodesic lies in an equatorial plane.

Hint: A geodesic lies in an equatorial plane when $\vartheta = \pi/2$ all along it, so $\dot\vartheta \equiv 0$. This means that $\Theta(\vartheta) \equiv 0$ in (17.50). So, to solve the problem one must find the solutions of the equation $\Theta(\vartheta) = 0$ with K obeying (17.57). There are two solutions: one is $\cos\vartheta = 0$, the other is

$$\sin^2\vartheta = \frac{{L_z}^2}{a^2\,(E^2 - {\mu_0}^2)}. \tag{17.84}$$

Calculate $\ddot\vartheta$ for both of these solutions by differentiating $\Sigma\dot\vartheta = \pm\sqrt{\Theta(\vartheta)}$, which follows from (17.50). Note that $\dot\vartheta/\sqrt{\Theta(\vartheta)}$, which will appear in the calculation, has a finite limit at $\dot\vartheta \to 0$ in both solutions of $\Theta(\vartheta) = 0$, equal to $\pm 1/\Sigma$. For $\cos\vartheta = 0$, $\ddot\vartheta = 0$, which means that $\cos\vartheta = 0$ holds all along the orbit. For (17.84), $\ddot\vartheta \neq 0$, so it holds only at one point of the orbit, and ϑ has an extremum there.